Motuporamines, Anti-Invasion and Anti-Angiogenic Alkaloids from the Marine Sponge *Xestospongia exigua* (Kirkpatrick): Isolation, Structure Elucidation, Analogue Synthesis, and Conformational Analysis

David E. Williams,[†] Kyle S. Craig,[†] Brian Patrick,[‡] Lianne M. McHardy,[§] Rob van Soest,[||] Michel Roberge,[§] and Raymond J. Andersen*[,†]

Departments of Chemistry, Oceanography (EOS), Biochemistry and Molecular Biology, University of British Columbia, Vancouver, British Columbia, Canada, and Department of Coelenterates and Porifera, Zoologisch Museum, University of Amsterdam, Amsterdam, The Netherlands

randersn@interchange.ubc.ca

Received September 8, 2001

Extracts of the sponge *Xestospongia exigua* collected in Papua New Guinea were positive in a new assay for anti-invasion activity. Bioassay-guided fractionation led to the identification of the three known motuporamines A (**1**), B (**2**), and C (**3**) along with the new motuporamines D (**4**), E (**5**), and F (**6**) and a mixture of G, H, and I (**15**). Motuporamines A (**1**), B (**2**), and C (**3**) and the mixture of G, H, and I (**15**) were responsible for the anti-invasion activity of the crude extract. Motuporamine C (**3**) has also been found to be anti-angiogenic. A series of analogues of the motuporamines have been synthesized and evaluated for anti-invasive activity. These SAR results revealed that a saturated 15-membered cyclic amine fused to the natural motuporamine diamine side chain (**13**) represented the optimal structure for anti-invasive activity in this family. Single-crystal X-ray diffraction analysis of one of the analogues **20** showed that in the solid state its 16-membered macrocyclic amine fragment adopted the [4444] quadrangular conformation predicted by calculations to be the lowest energy conformation for the corresponding cycloalkane, cyclohexadecane. These data along with literature X-ray data and conformational analysis for derivatives of azacyclotridecane have been used as precedents for predicting the lowest energy ring conformations of other motuporamines. The SAR data from the natural and synthetic motuporamines have been combined with the conformational analyses to provide an outline of the functionality and shape required for activity in this family of alkaloids and to design a new analogue **49** that showed good anti-invasion activity.

Introduction

The ability of tumor cells to invade adjacent tissue through the extracellular matrix is critical to metastasis, the process by which a tumor cell leaves the primary tumor, travels to a distant site via the circulatory system, and establishes a secondary tumor.[1] Metastasis is the main cause of death in cancer patients and a major impediment to improving cures. Tumors also stimulate angiogenesis, the formation of new blood vessels.[2] Without the formation of new blood vessels, tumors cannot increase in size and they cannot metastasize. Angiogenesis, which requires migration of vascular endothelial cells through the extracellular matrix toward tumors, shares many features with tumor invasion. Therefore, inhibition of extracellular matrix invasion represents an attractive chemotherapeutic approach to preventing metastasis and angiogenesis. This approach has the advantage that the steps required for metastasis and angiogenesis are similar for all tumor cell types regardless of the genetic basis for the tumor origin. Consequently, chemical agents that block metastasis and angiogenesis by inhibiting invasion should be useful in treating cancers of various genetic origins. An additional potential advantage of this form of treatment is the fact that angiogenesis does not occur under normal physiological conditions in adults, except for wound healing and some portions of the female reproductive cycle, so side effects should be minimal if the treatment is highly selective.

The promise of anti-angiogenic/anti-metastatic therapy has attracted a lot of attention, and a number of drugs with one or both of these properties are in various stages of pre-clinical and clinical evaluation.[2b−d] Included in this group are the fumagilin analogue TNP-470,[3] thalidomide,[4] endostatin,[5] SU5416,[6] marimastat,[7] AG3340,[8]

[†] Departments of Chemistry and Oceanography (EOS), University of British Columbia.

[‡] Department of Chemistry, University of British Columbia.

[§] Department of Biochemistry and Molecular Biology, University of British Columbia.

[||] University of Amsterdam.

(1) (a) Wyke, J. A. *European Journal of Cancer* **2000**, *36*, 1589−1594.)b) Zetter, B. R. *Annu. Rev. Med.* **1998**, *49*, 407−424. (c) Woodhouse, E. C.; Chuaqui, R. F.; Liotta, L. A. *Cancer* (Suppl.) **1997**, *80*, 1529−1537.

(2) (a) Folkman, J. *N. Engl. J. Med.* **1971**, *285*, 1182−1186. (b) Carmeliet, P.; Jain, R. *Nature* **2000**, *407*, 249−257. (c) Westphal, J. R.; Ruiter, D. J.; De Waal, R. M. W. Int. *J. Cancer* **2000**, *86*, 870−873. (d) Liekens, S.; De Clerq, E.; Neyts, J. *Biochem. Pharmacol.* **2001**, *61*, 253−270.

(3) Ingber, D.; Fujita, T.; Kishimoto, S.; Sudo, K.; Kanamarau, T.; Brem, H.; Folkman, J. *Nature* **1990**, *348*, 555−557.

(4) D'Amato, R. J.; Loughnan, M. S.; Flynn, E.; Folkman, J. *Proc. Natl. Acad. Sci. U.S.A.* **1994**, *91*, 4082−4085.

(5) O'Reilly, M. S.; Boehm, T.; Shing, Y.; Fukai, N.; Vasios, G.; Lnae, W. S.; Flynn, E.; Birkhead, J. R.; Olsen, B. R.; Folkman, J. *Cell* **1997**, *88*, 277−285.

10.1021/jo016101c CCC: $22.00
Published on Web 12/12/2001

neovastat,[9] interferon-α,[10] a combretastatin A-4 prodrug,[11] and squalamine.[12] While some of these compounds are showing preliminary indications of clinical promise, there is still a serious need to identify and evaluate additional anti-angiogeneic and anti-metastatic drugs. Toward this end, we have developed a quantitative assay suitable for testing crude natural extracts for inhibitors of extracellular matrix invasion.[13] The assay, which uses highly invasive metastatic MDA-231 breast carcinoma cells, is simple to carry out yet has the advantage of eliminating cytotoxicity and inhibition of extracellular matrix attachment as causes of invasion inhibition.

An initial screening of ~250 crude extracts of tropical marine invertebrates in the assay resulted in the identification of one active hit. The source organism for this hit was the marine sponge *Xestospongia exigua* collected in the waters off the coast of Papua New Guinea. Bioassay-guided fractionation of the crude extract led to the identification of the three known motuporamines, A (**1**), B (**2**), and C (**3**),[14] and the new motuporamines D (**4**), E (**5**), F (**6**), G, H, and I. Motuporamines A (**1**), B (**2**), and C (**3**) and the mixture of G, H, and I (i.e., **15**) were primarily responsible for the anti-invasion activity of the crude extract. Follow-up assays have shown that motuporamine C (**3**) is also active in an in vitro HUVEC sprouting assay and in an in vivo CAM assay for anti-angiogenic activity.[13] An in vitro "wound-healing" assay has shown that the motuporamines work by inhibiting cell motility.[13] The motuporamines represent a novel structural class of anti-invasion and anti-angiogenic natural products. Herein, we report the details of the isolation and structure elucidation of the motuporamines, details of the synthesis and biological activities of a series of analogues of the natural products, and a conformational analysis of several members of the family, which has provided an outline of the functionality and shape required for anti-invasion activity in this family of alkaloids.

Results

Isolation and Structure Elucidation of the Motuporamines. Specimens of *X. exigua* were collected by hand using scuba on the outer reef at Motupore Island, Papua New Guinea. Freshly collected sponge samples were frozen on site and transported to Vancouver over dry ice where they were thawed and extracted repeatedly with MeOH. The concentrated MeOH soluble materials were partitioned between H_2O and EtOAc resulting in an anti-invasive aqueous-soluble fraction and an inactive EtOAc-soluble fraction. Further partitioning of the bioactive H_2O-soluble materials between H_2O and *n*-butanol resulted in the anti-invasion activity being concentrated in the *n*-butanol. Repeated Sephadex LH20 chromatography of the *n*-butanol-soluble materials using first MeOH and subsequently 20:5:2 EtOAc/MeOH/H_2O as eluents gave a glassy solid that contained only a mixture of the motuporamines and was active in the anti-invasion assay. Reversed-phase HPLC was used to separate the mixture of motuporamines into pure samples of motuporamines A (**1**), B (**2**), C (**3**), D (**4**), and E (**5**) and a fraction that contained an inseparable mixture of motuporamines G, H, and I. The major component of the mixture was motuporamine C (**3**) with all the other analogues being present in less than 10% of its concentration. Monoacetylmotuporamine C (**7**) and monotrifluroacetylmotuporamine C (**8**), which are both presumed to be isolation artifacts, were also obtained from the HPLC fractionation. The mixture of G, H, and I was resolved by acetylating the mixture, separating the diacetylated derivatives via reversed phase HPLC, removing the acetyl groups by HCl catalyzed hydrolysis, and then purifying the individual alkaloids by reversed phase HPLC to give motuporamines G, H, and I as single compounds. Motuporamine F (**6**) was only isolated as its diacetyl derivative **9** during fractionation of a sample of the motuporamine mixture that had been acetylated prior to HPLC purification.

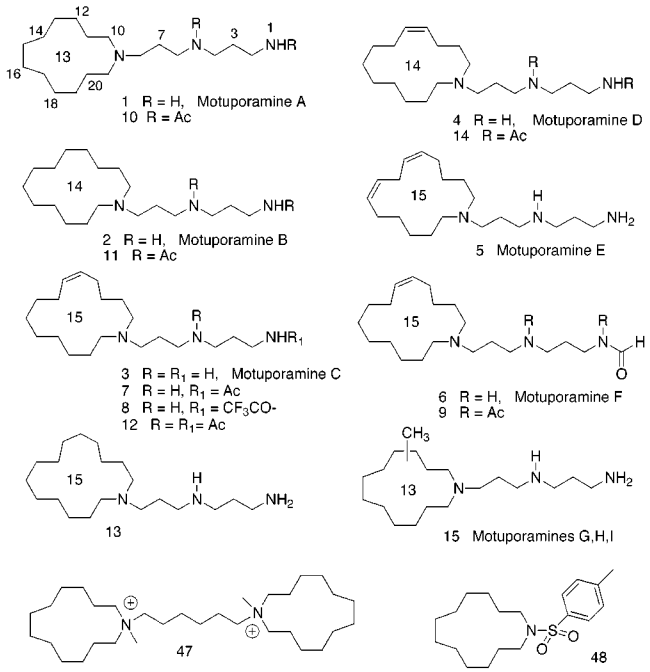

Motuporamine A (**1**) was obtained as a pale yellow oil that gave an $[M + H]^+$ ion at *m*/*z* 298.3229 in the positive-ion HRFABMS appropriate for a molecular formula of $C_{18}H_{39}N_3$, requiring one site of unsaturation. The ^{13}C NMR spectrum (Table 2) obtained for **1** contained only 12 resonances, all with chemical shifts between δ 22.4 and 53.5 ppm, which indicated that there was an element of symmetry in the molecule and that the site of unsaturation was a ring. Five of the carbon resonances had chemical shifts (δ 37.8, 46.0, 46.1, 53.1, and 53.5 ppm) typical of aliphatic methylenes attached to nitrogen. One

(6) Rosen, L.; Rosen, P.; Amado, R.; Chang, D.; Mulay, M.; Parson, M.; Laxa, B.; Langecker, P.; Gracey, S.; Siek, A.; Hannah, A. *Clinical Cancer Research* **1999**, *5* (Suppl.), 13.

(7) Steward, W. P. *Cancer Chemother. Pharmacol.* **1999**, *43* (Suppl.), S56−S60.

(8) Shalinsky, D. R.; Brekken, J.; Zou, H.; McDermott, C. D.; Forsyth, P.; Edwards, D.; Margosiak, S.; Bender, S.; Truitt, G.; Wood, A.; Varki, N. M.; Appelt, K. *Ann. NY Acad. Sci.* **1999**, *878*, 236−270.

(9) Riviere, M.; Latreille, J.; Falardeau, P.; Dupont, E. *Ann. Oncol.* **1998**, *9* (Suppl. 4), 636pp.

(10) Sidky, Y. A.; Borden, E. C. *Cancer Res.* **1987**, *47*, 5155−5161.

(11) Chaplin, D. J.; Pettit, G. R.; Hill, S. A. *Anticancer Res.* **1999**, *19*, 189−195.

(12) Sills, A. K.; Williams, J. I.; Tyler, B. M.; Epstein, D. S.; Sipos, E. P.; Davis, J. D.; McLane, M. P.; Pitchford, S.; Cheshire, K.; Gannon, F. H.; Kinney, W. A.; Chao, T. L.; Donowitz, M.; Laterra, J.; Zasloff, M.; Brem, H. *Cancer Res.* **1998**, *58*, 2784−2792.

(13) Roskelley, C. D.; Williams, D. E.; McHardy, L. M.; Leong, K. G.; Troussard, A. Karsan, A.; Andersen, R. J.; Dedhar, S.; Roberge, M. *Cancer Res.* **2001**, *61*, 6788−6794.

(14) Williams, D. E.; Lassota, P.; Andersen, R. J. *J. Org. Chem.* **1998**, *63*, 4838−4841.

Table 1. ^{1}H NMR Data for Motuporamines A (1), B (2), C (3), D (4), E (5), 7, and 8 and Diacetylmotuporamine F (9) Recorded in MeOH-d_4 at 500 MHz

atom	1	2	3	4	5	7	8	9
2	3.05, t, J = 7.6, 2H	3.05, t, J = 7.6 2H	3.04, t, J = 7.2 2H	3.06, t, J = 7.4 2H	3.05, m 2H	3.30, m 2H	3.40, t, J = 6.7 2H	3.71, t, J = 7.4 1H 3.16, 1H
3	2.08, m, 2H	2.09, m, 2H	2.08, m, 2H	2.10, m, 2H	2.09, m, 2H	1.86, m, 2H	1.96, m, 2H	1.82, m, 2H
4	3.11−3.17	3.11−3.23	3.10−3.16	3.17	3.16	3.02, t, J = 6.9 2H	3.05, m, 2H	3.38, m, 2H
6	3.11−3.17	3.11−3.23	3.10−3.16	3.14	3.14	3.08, t, J = 7.4 2H	3.10, m, 2H	3.41, m, 2H
7	2.17, m, 2H	2.17, m, 2H	2.15, m, 2H	2.17	2.18	2.15, m, 2H	2.15, m, 2H	2.00, m, 2H
8	3.25, m, 2H	3.26, m, 2H	3.25, m, 2H	3.25, m, 2H	3.25, m, 2H	3.27, m, 2H	3.24, m, 2H	3.10−3.15
10	3.11−3.17	3.11−3.23	3.10−3.16	3.14	3.18	3.14, m, 2H	3.15, m, 2H	3.10−3.15
11	1.76, m, 2H	1.69, m, 2H	1.69, m, 2H	1.64, m, 2H	1.68, m, 2H	1.71, m, 2H	1.71, m, 2H	1.71, m, 2H
12	1.41−1.53	1.36−1.53	1.43	2.13	1.56, m, 2H	1.43, m, 2H	1.35−1.45	1.50−1.58
13	1.41−1.53	1.36−1.53	2.15, m, 2H	5.54, m, 1H	2.18	2.16, m, 2H	2.15, m, 2H	2.15, m, 2H
14	1.41−1.53	1.36−1.53	5.31, m, 1H	5.40, m, 1H	5.27, m, 1H	5.32, m, 1H	5.32, m, 1H	5.33, m 1H
15	1.41−1.53	1.36−1.53	5.36, m, 1H	2.15	5.48, m, 1H	5.38, m, 1H	5.38, m, 1H	5.39, m, 1H
16	1.41−1.53	1.36−1.53	2.15, m, 2H	1.52	2.88, m, 2H	2.13, m, 2H	2.15, m, 2H	2.15, m, 2H
17	1.41−1.53	1.36−1.53	1.48	1.35	5.52, m, 1H	1.49, m, 2H	1.50	1.50
18	1.41.1.53	1.36−1.53	1.33	1.37	5.29, m, 1H	1.35, m, 2H	1.34	1.35
19	1.41.1.53	1.36−1.53	1.43[a]	1.39	2.16	1.43, m, 2H	1.35−1.45	1.44[a]
20	1.76, m	1.36−1.53	1.33[a]	1.52	1.53, m, 2H	1.35, m, 2H	1.35−1.45	1.35[a]
21	3.11−3.17	1.69, m, 2H	1.46	1.75, m, 2H	1.40, m, 2H	1.46, m, 2H	1.47	1.44−1.49
22		3.11−3.23	1.69, m, 2H	3.14	2.14	1.71, m, 2H	1.71, m, 2H	1.71, m, 2H
23			3.10−3.16		3.10	3.14, m, 2H	3.13, m, 2H	3.10−3.15
N1								
Me						1.97, s, 3H		2.43, s, 3H
C*H*O								9.20, s, 1H
N5								
Me								2.13, s, 3H

[a] Assignments within a column are interchangeable. Assignments and some chemical shifts are based on HMQC, HMBC and COSY data.

Table 2. ^{13}C NMR Data for Motuporamines A (1), B (2), C (3), D (4), E (5), 7, and 8 and Diacetylmotuporamine F (9) Recorded in MeOH-d_4 at 100 MHz

atom	1	2	3	4	5	7	8	9
2	37.8	37.8	37.8	37.8	37.8	36.7	37.6	37.8
3	25.4	25.4	25.4	25.5	25.4	27.8	27.1	28.1
4	46.0	46.0	46.0[a]	46.0	46.0	46.4	46.6	48.0
6	46.0	46.0	45.9[a]	46.0	46.0	45.8	45.9	43.9
7	22.5	22.7	22.5	22.8	22.6	22.5	22.5	24.2
8	53.1	52.6	53.4[b]	52.4	52.9	53.4	53.4	53.9
10	53.5	51.6	53.9[b]	51.7	52.6	53.9	54.0	53.6
11	22.4	20.5	23.6	24.7[a]	22.3	23.7	23.7	23.7
12	25.3	24.2	26.5[c]	24.8	25.9	26.6	26.6	26.6
13	26.7[a]	26.4[a]	27.0	128.4	26.7	27.0	27.0	27.0
14	25.9[a]	24.8[a]	130.5	133.5	129.8	130.5	130.5	130.5
15	25.7[a]	25.3[a]	133.1	25.9	131.3	133.1	133.2	133.1
16	25.7[a]	27.0	26.4[c]	28.4	27.0	26.5	26.5	26.6
17	25.9[a]	25.3[a]	29.2	27.9	130.1	29.2	29.2	29.2
18	26.7[a]	24.8[a]	27.8	25.8	130.2	27.9	27.9	27.8
19	25.3	26.4[a]	27.4[c]	26.3	25.8	27.5	27.4[a]	27.5[a]
20	22.4	24.2	27.0[c]	24.6[a]	27.8	27.0	27.0[a]	27.0[a]
21	53.5	20.5	24.9	19.1	24.7	25.0	25.0	25.0
22		51.6	23.0	50.3	22.9	23.1	23.1	23.2
23			53.1[b]		53.2	53.1	53.2	52.9
N1								
*C*O						174.8	159.7	173.6
Me						22.4		22.6
*C*HO								165.4
N5								
*C*O								174.4
Me								21.3

[a−c] Assignments within a column are interchangeable. Assignments and some chemical shifts are based on HMQC, HMBC and COSY data.

of these resonances at δ 53.5 was twice the intensity of the others, suggesting that it accounted for two chemically equivalent carbons. The HRFABMS and ^{13}C NMR data described above for **1** suggested that the molecule was motuporamine A, which had previously been isolated from *X. exigua* but only as its diacetylated derivative **10**.[14] To confirm this assignment, **1** was reacted with acetic anhydride in pyridine at rt, which gave a quantitative yield of diacetylmotuporamine A (**10**) that was identical to the original sample by HPLC, NMR, and MS comparison.

Motuporamine B (**2**) was obtained as an amorphous solid that gave an $[M + H]^+$ ion at m/z 312.3387 in the positive-ion HRFABMS appropriate for a molecular formula of $C_{19}H_{41}N_3$. The ^{13}C NMR spectrum obtained for **2** (Table 2) showed a strong resemblance to the ^{13}C spectrum of **1** except that it contained three-half intensity resonances in the region of δ 20 to 28 ppm compared to only two in the spectrum of **1**. This observation suggested that compound **2** was motuporamine B, which differs from motuporamine A (**1**) simply by having one additional methylene in the macrocyclic amine fragment. Treatment of **2** with acetic anhydride in pyridine at rt converted it to **11**, which was identical to authentic diacetylmotuporamine B.[14]

Motuporamine C (**3**) was isolated as an amorphous solid that gave an $[M + H]^+$ ion at m/z 324.3381 in the positive-ion HRFABMS appropriate for a molecular formula of $C_{20}H_{41}N_3$, requiring two sites of unsaturation. The ^{13}C NMR spectrum obtained for **3** (Table 2) contained 20 resolved resonances demonstrating that it lacked the symmetry found in motuporamines A (**1**) and B (**2**). A pair of methine resonances at δ 130.5 and 133.1 ppm identified a disubstituted olefin as one site of unsaturation and the lack of ^{13}C NMR evidence for other sites of unsaturation required the presence of a ring. The HRFABMS and ^{13}C NMR data for **3** suggested that the compound was motuporamine C, previously isolated only as its diacetyl derivative **12**.[14] Acetylation of **3** gave a quantitative yield of **12**, identical in all respects to the original material, confirming the assignment. In the initial report of diacetylmotuporamine C (**12**), there was an unresolved ambiguity about the position of the olefin in the macrocyclic amine fragment. This was subse-

quently resolved by Goldring and Weiler through an unambiguous total synthesis of both possible isomers.[15] Motuporamine C (**3**) was hydrogenated to give dihydromotuporamine C (**13**) for biological testing. The structures of monoacetylmotuporamine C (**7**) and monotrifluroacetylmotuporamine C (**8**), both obtained in small amounts from the HPLC fractionation, were routinely assigned by analysis of their spectroscopic data. Monoacetylmotuporamine C (**7**) is presumed to be an artifact resulting from reaction of motuporamine C (**3**) with EtOAc during the solvent partitioning step and monotrifluroacetylmotuporamine C (**8**) is presumed to have formed by reaction of **3** with the TFA used as a solvent modifier in the reversed phase HPLC fractionation.

Motuporamine D (**4**) was isolated as a colorless oil that gave an $[M + H]^+$ ion at *m/z* 310.3212 in the positive-ion HRFABMS appropriate for a molecular formula of $C_{19}H_{39}N_3$ requiring two sites of unsaturation. The ^{13}C NMR spectrum of **4** (Table 2) contained eighteen resolved resonances and HMQC correlations showed that a resonance at δ 46.0 accounted for two nonequivalent methylene carbons, in agreement with the HRFABMS data. A pair of olefinic methine resonances at δ 128.4 and 133.5, assigned to a disubstituted olefin, accounted for one of the sites of unsaturation and the absence of ^{13}C NMR evidence for other unsaturated functionality indicated the presence of a ring. Six of the aliphatic methylene resonances in the ^{13}C NMR spectrum of **4** had chemical shifts (δ 37.8 (C-2), 25.5 (C-3), 46.0 (C-4), 46.0 (C-6), 22.8 (C-7), 52.4 (C-8)) virtually identical to those assigned to the spermidine-like side chain of motuporamine C (**3**) (δ 37.8 (C-2), 25.4 (C-3), 46.0 (C-4), 45.9 (C-6), 22.5 (C-7), 53.4 (C-8)), demonstrating that **4** contained an identical side chain fragment. The ^1H NMR spectrum of **4** showed no evidence for methyl residues. Therefore, it was apparent that motuporamine D (**4**) contained a mono-olefinic 14-membered macrocyclic amine attached to the spermidine-like side chain. The location of the olefin was determined by analysis of the COSY spectrum of diacetylmotuporamine D (**14**). A well-dispersed methylene resonance at δ 1.64 (H-11) showed COSY correlations to a pair of resonances at δ 3.11 and 3.27 (H-10) and to another methylene resonance at δ 2.10−2.19 (H-12), which was in turn correlated to the olefinic methine resonance at δ 5.53 (H-13). The methylene resonances at δ 3.11 and 3.27 (H-10) were assigned to protons on a carbon attached to nitrogen by their HMQC correlation to a carbon at δ 51.7. This set of correlations demonstrated that there were three methylene carbons separating the nitrogen in the macrocyclic amine from the olefin. Simultaneous irradiation of the H-12 (δ 2.13) and H-15 (δ 2.15) methylene protons simplified each of the H-14 (δ 5.40) and H-13 (δ 5.54) resonances to doublets with J = 11 Hz indicating that the $\Delta^{13,14}$ olefin had the *Z* configuration.

Motuporamine E (**5**) was isolated as a colorless oil that gave a $[M + H]^+$ ion at *m/z* 322.3226 in the positive-ion HRFABMS corresponding to a molecular formula of $C_{20}H_{39}N_3$, requiring three sites of unsaturation. Examination of the ^1H and ^{13}C NMR data for **5** (Tables 1 and 2) showed that it had the same skeleton as motuporamine C (**3**) but contained two olefins in the macrocylic amine. A two-proton ^1H NMR resonance at δ 2.88 (H-16), whose chemical shift was consistent with a doubly allylic methylene residue, showed COSY correlations to a two-proton olefinic resonance at δ 5.48−5.52 (H-15/H-17), indicating that the two olefins were separated by a single methylene carbon. Starting with the other olefinic resonance (δ 5.27−5.29 (H-14/H-18)) it was possible to trace a sequential series of COSY correlations to H-13 (δ 2.18), H-12 (δ 1.56), H-11 (δ 1.68), and H-10 (δ 3.18). The chemical shift of the H-10 resonance (δ 3.18) was consistent with protons attached to a carbon bonded to nitrogen. Therefore, it was apparent that in motuporamine E (**5**) there were four methylene carbons separating the first olefin from the macrocylic amine nitrogen, as in motuporamine C (**3**). Irradiation of the doubly allylic methylene resonance at δ 2.88 (H-16) simplified the H-15 and H-17 olefinic resonances (δ 5.52 and 5.58) to doublets with J = 11 Hz indicating that both the $\Delta^{15,16}$ and $\Delta^{17,18}$ olefins had the *Z* configuration.

Diacetylmotuporamine F (**9**) was obtained in small quantities as a colorless oil from a mixture of motuporamines that was acetylated prior to fractionation. It gave an $[M + H]^+$ ion at *m/z* 436.3538 in the positive-ion HRFABMS corresponding to a molecular formula of $C_{25}H_{46}N_3O_3$. The ^1H and ^{13}C NMR data obtained for **9** (Tables 1 and 2) showed a striking resemblance to the data for diacetylmotuporamine C (**12**), indicating that the two molecules were closely related. A proton resonance at δ 9.20 was correlated to a carbon resonance at δ 165.4 in the HMQC spectrum of **9** indicating that there was a formamide residue in **9** that was not present in **12**. In the HMBC spectrum, a methylene resonance at δ 3.71, assigned to H-2, was correlated to the formamide carbonyl resonance at δ 165.4 and also to an acetamide carbonyl resonance at δ 173.6, indicating that both acyl residues were attached to N-1. Further support for this assignment came from the presence of an HMBC correlation between the formamide proton resonance (δ 9.20) and the acetamide carbonyl resonance (δ 165.4). Both the formamide proton and N-1 acetamide methyl resonances were split into two peaks in a ratio of ~4:1 presumably reflecting the presence of slowly interconverting formamide rotamers.

Motuporamines G, H, and I were all obtained in very small quantities. Each of them gave $[M + H]^+$ ions in the HRFABMS that corresponded to molecular formulas of $C_{19}H_{41}N_3$. Analysis of the NMR data obtained for each compound showed that they were all members of the motuporamine family with the same spermidine-like diamine side chain found in all the other natural analogues and that they also had a saturated macrocyclic amine fragment. The feature that set motuporamines G, H, and I apart was the presence of a doublet methyl resonance at δ ~0.98 in the ^1H NMR spectrum of each, which could only be assigned to a methyl branch in the macrocyclic amine of each compound, making them methylated analogues of motuporamine A (**1**). The proton NMR spectra of the free amine forms of motuporamines G, H, and I as well as the proton NMR spectra of the corresponding diacetamides exhibited very broad signals

(15) Goldring, W. P. D.; Weiler, L. *Org. Lett.* **1999**, *1*, 1471−1473.

(16) Baldwin, J. E.; Vollmer, H. R.; Lee, V. *Tetrahedron Lett.* **1999**, *40*, 5401−5404.

(17) Furstner, A.; Rumbo, A. *J. Org. Chem.* **2000**, *65*, 2608−2611.

(18) Rubin, B. H.; Williamson, M.; Takeshita, M.; Menger, F. M.; Anet, F. A. L.; Bacon, B.; Allinger, N. L. *J. Am. Chem. Soc.* **1984**, *106*, 2088−2092.

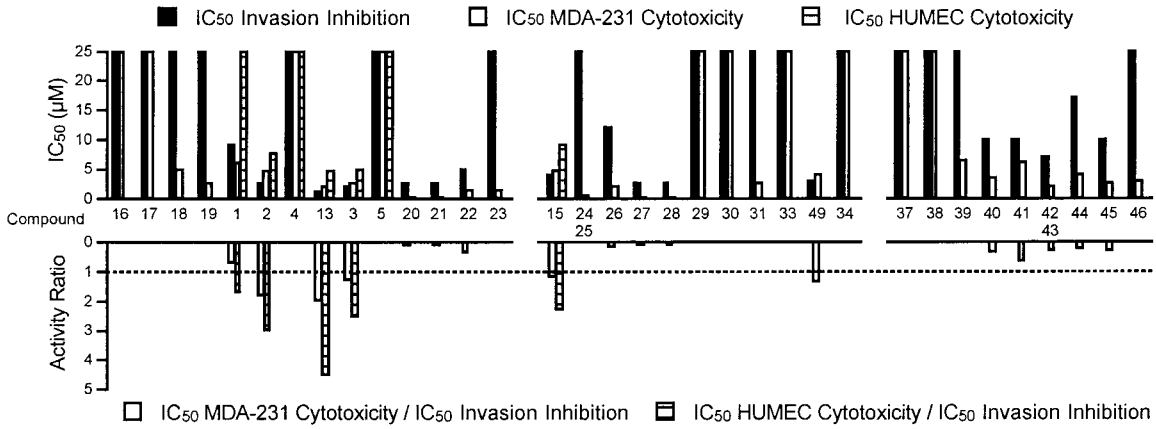

Figure 1. Anti-invasion and cytotoxicity data for natural and synthetic motuporamines. The upper panel shows the IC_{50} for inhibition of matrigel invasion by MDA-231 cells and cytotoxicity toward MDA-231 and HUMEC cells. Values higher than 25 μM are shown as 25 μM. The activity ratio of the compounds active in the anti-invasion assay is shown in the lower panel as the ratio of the IC_{50} for invasion inhibition to the IC_{50} for cytotoxicity to MDA-231 or HUMEC cells. The dashed line indicates a ratio of 1.

that could not be sharpened by changing the acquisition temperature or solvent. As a consequence, it has not been possible to determine the exact location of the methyl branch in each compound, although it was possible to rule out methyl branches at C-10 and C-11. Since there are three distinct isomers, they must each have general structure **15** where the branches are individually located between C-12 and C-15.

Figure 1 (upper panel) shows the IC_{50}'s for the natural motuporamines in the invasion assay. Motuporamines A (**1**), B (**2**), and C (**3**), a mixture of motuporamines G, H, and I (**15**), and dihydromotuporamine C (**13**) all showed significant activity in the assay (IC_{50}'s < 15 μM). The mono-olefinic motuporamine D (**4**), the diene motuporamine E (**5**), as well as all the diacetylated derivatives were inactive.

Synthetic Analogues of Motuporamines. The invasion inhibition activity of the naturally occurring motuporamines and a few simple derivatives of them provided some preliminary insight into the structural requirements for activity in this family of alkaloids. Motuporamines A (**1**) and B (**2**) and dihydromotuporamine C (**13**) form a series that differs only in the size of the macrocyclic amine. There is a general trend toward increasing potency as the ring size increases from 13 to 15 atoms in this group (Figure 1). Motuporamine C (**3**), which has a single olefin in the macrocycle, is only slightly less potent than the reduced form **13**, while motuporamine E (**5**), which has the same ring size as motuporamine C (**3**) but has a diene in the macrocycle, is inactive. Diacetylmotuporamine C (**12**), like all of the other diacetyl motuporamine derivatives, is inactive.

The SAR data obtained from the natural products illustrates that subtle changes to either the macrocyclic amine or to the diamino side chain in the motuporamines can lead to significant reduction in activity. To gain a deeper understanding of the structural requirements for anti-invasion and anti-angiogenic activity in this class of compounds, we have synthesized a number of analogues. The first objective of the synthetic program was to probe the effects of changing the macrocyclic amine fragment by (i) varying the ring size, (ii) replacing the ring completely with two linear saturated alkyl chains that in total had approximately the same number of carbons as active motuporamines, and (iii) replacing the macrocyclic amine with a variety of commercially available polycyclic and partially aromatic amines with roughly comparable carbon numbers to active motuporamines. A second objective of the synthetic program was to vary the diamino side chain by (i) changing the spacing between the amines and (ii) changing the number of amines.

There are three literature reports of the total synthesis of motuporamines that provided the basic methodology required for the analogue synthesis program.[15−17] Each of the syntheses starts by preparing either a saturated or mono-olefinic macrocyclic amine, which is then fused with the spermidine-like side chain. In two of the syntheses, the macrocyclic amines are prepared by reduction of macrocyclic lactams that are either commercially available, prepared by Beckman rearrangement of a oxime formed from a macrocylic ketone precursor,[16] or prepared via ring-closing olefin metathesis reactions of linear secondary amides.[15] The third synthesis prepares mono-olefinic macrocyclic amines with the Z configuration via a ring-closing alkyne metathesis reaction on a Fmoc-protected acyclic secondary amine.[17] Two of the syntheses add the side chain to the macrocylic amine via a reductive amination sequence.[16,17] The Goldring and Weiler synthesis adds the macrocyclic amine to methylacrylate in a Michael reaction, followed by amide formation between the resulting methyl ester and 1,3-diaminopropane, and finally reduction of the newly formed secondary amide with LAH to give motuporamines.[15]

Schemes 1 and 2 show the reaction sequences used to prepare motuporamine analogues with saturated 5- (**16**), 6- (**17**), 9- (**18**), 11- (**19**), 16- (**20**), and 18-membered (**21**) cyclic amine fragments (see Chart 1 for structures). The lactams required for making the 11- and 16-membered cyclic amines **19** and **20** were prepared by Beckman ring expansions of the 10- and 15-membered cyclic ketones, respectively (Scheme 1B), and the lactams required for making the 18-membered cyclic amine analogues **21**, **22**, and **23** were prepared by ring-closing olefin metathesis followed by catalytic hydrogenation (Scheme 2). A pair of dimeric lactams resulting from intermolecular coupling in the olefin metathesis reaction gave small amounts of the side products **24** and **25** in the synthesis of the 18-membered motuporamine analogue **21**. The use of dihexylamine, dioctylamine, and didecylamine in place of

Scheme 1

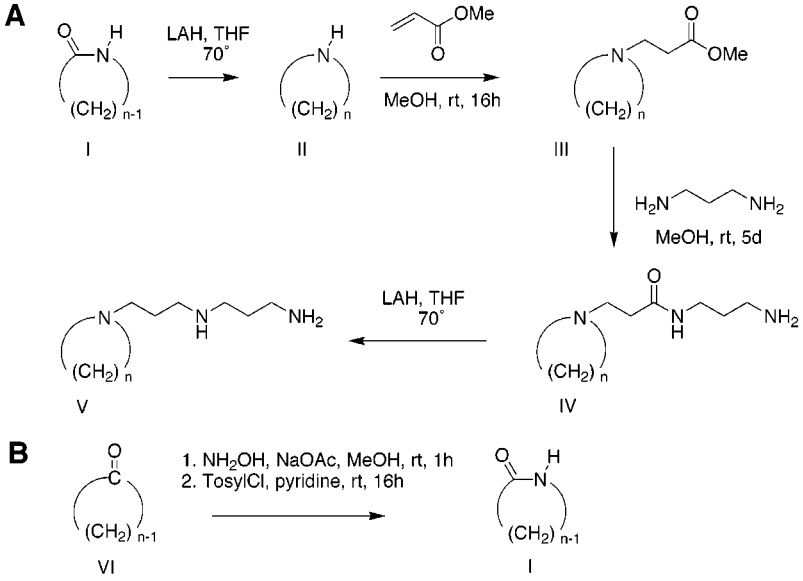

Scheme 2

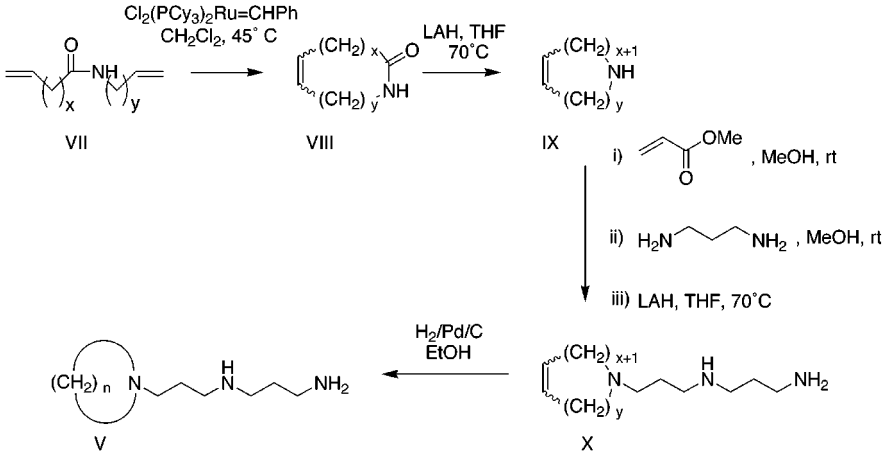

the cyclic amine **II** in Scheme 1A led to the formation of the three acyclic motuporamine analogues **26**, **27**, and **28**, respectively.

Two bicyclic motuporamine analogues **29** and **30** were prepared according to Scheme 1A using tetrahydroisoquinoline and decahydroquinoline as the cyclic amine intermediates **II**. LAH reduction of 4-azatricyclco[4.3.1.1^{3,8}]-undecano-5-one gave the corresponding tricyclic amine that was converted via Scheme 1A into the tricyclic motuporamine analogue **31**. Similarly, the crown ether **32** was converted to the motuporamine analogue **33** in good yield.

The 13-membered cyclic amine fragment **34** of motuporamine A (**1**) was used as the scaffold for preparation of a series of side-chain modified analogues as shown in Scheme 3 because the required precursor lactam **35** was readily available. Addition of ammonia, *n*-butylamine, 3-amino-1-propanol, 1,2-diaminoethane, 1,4-diamino-*n*-butane, and spermidine to the methyl ester **36** (Scheme 3b) followed by reduction of the newly formed amide with LAH gave the motuporamine A analogues **37**, **38**, **39**, **40**, and **41**, and a mixture of **42** and **43**, respectively, all in good yield. Modification of the Goldring and Weiler synthesis, as shown in Scheme 3a, by replacing methyl acrylate with methylchloroacetate, methyl-4-iodobutyrate, and ethyl-6-bromohexanoate resulted in the formation of the motuporamine A analogues **44**, **45**, and **46** where the ring nitrogen and the adjacent side chain nitrogen were separated by two, four, and six methylene carbons, respectively.

Anti-Invasion and Cytotoxic Activities of Natural Motuporamines and the Synthetic Analogues. The biological activity of the natural motuporamines and the synthetic analogues was evaluated in three in vitro assays. Anti-invasion activity was measured using the new MDA-231 breast carcinoma cell assay,[13] and the results are reported in Figure 1 (solid bars) as IC_{50}'s in units of μM resulting from a 2.5 h exposure of test cells to each compound. The screen for anti-invasion compounds was designed to discover agents that were not overtly toxic during the 2.5 h assay period. The natural and synthetic motuporamine analogues were also screened for in vitro cytotoxicity by measuring their ability to inhibit proliferation of MDA-231 human breast carcinoma cells after a 24h exposure to each compound. The results are also reported in Figure 1 (hollow bars). The most promising compounds emerging from the two assays described above were then tested for their ability to inhibit proliferation of normal human mammary epithelial HUMEC cells after a 24 h exposure to each compound. The results are reported in Figure 1 (hatched bars).

Chart 1. Structures of Motuporamine Analogs with Variations in the Cyclic Amine Fragment

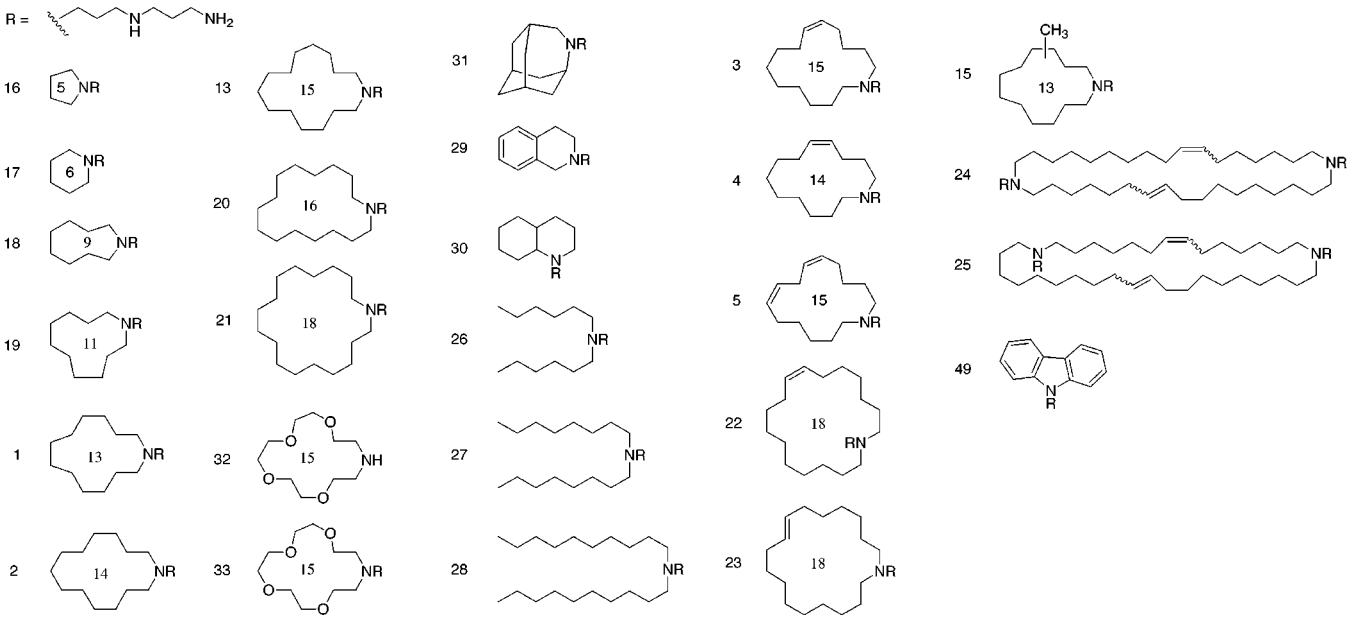

Scheme 3

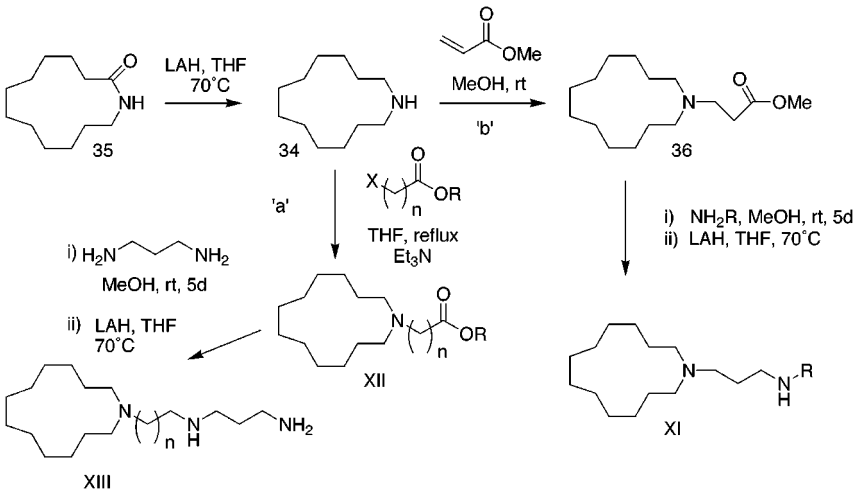

Conformations of Motuporamines. The goal of synthesizing analogues of the natural motuporamines was to determine the structural requirements for activity in this series of alkaloids. Another important piece of information for defining an anti-invasion/anti-angiogenic pharmacophore that could be used for designing analogues with improved activity is some knowledge about the conformation of the most active compounds. One of the central issues in the analysis of the conformation of the motuporamines is the shape of the macrocyclic amine. Although there is not much literature on the conformations of cyclic amines with ring sizes between 13 and 18 atoms, there are two reports of X-ray diffraction analyses of derivatives of the 13-membered cyclic amine. Allinger et al. reported the solid-state conformation of the dimeric compound **47**[18] and Sim has reported the solid-state conformation of N-(*p*-toluenesulfonyl)azacyclcotridecane (**48**).[19] In both cases, the macrocyclic ring adopts the [13333] conformation (Figure 2) calculated by Arnet et al.[20] to be the lowest energy conformation for the corresponding hydrocarbon cyclotridecane. The substituted nitrogen atom occupies a corner position in the solid-state [13333] conformation of both molecules **47** and **48** and the alkyl chain spacer in **47** is in a pseudoequatorial orientation that allows it to act as an extension of one of the straight all anti sides of the ring.

The proton NMR spectra obtained for the motuporamines were highly congested and gave rather broad signals making it impossible to analyze their solution conformations via NMR. Fortunately, the tris-trifluoroacetate salt of the 16-membered motuporamine analogue **20** gave large crystals allowing us to determine its solid-state conformation via X-ray diffraction analysis. Figure 3 shows two projections of a computer-generated ORTEP drawing of the solid-state conformation of **20** as determined by single-crystal X-ray diffraction analysis. Dale has used calculations to predict the most stable conformations of cycloalkanes with ring sizes up to 16 carbons. The solid-state conformation of the macrocyclic amine fragment in **20** is the [4444] quadrangular conformation shown in Figure 2 that was predicted by Dale[21] to be the

(19) Sim, G. A. *Acta Crystallogr.* **1987**, *C43*, 780−782.
(20) Anet, F. A. L.; Rawdah, T. N. *J. Am. Chem. Soc.* **1978**, *100*, 7810−7814.
(21) Dale, J. *Acta Chem. Scand.* **1973**, *27*, 1115−1129.

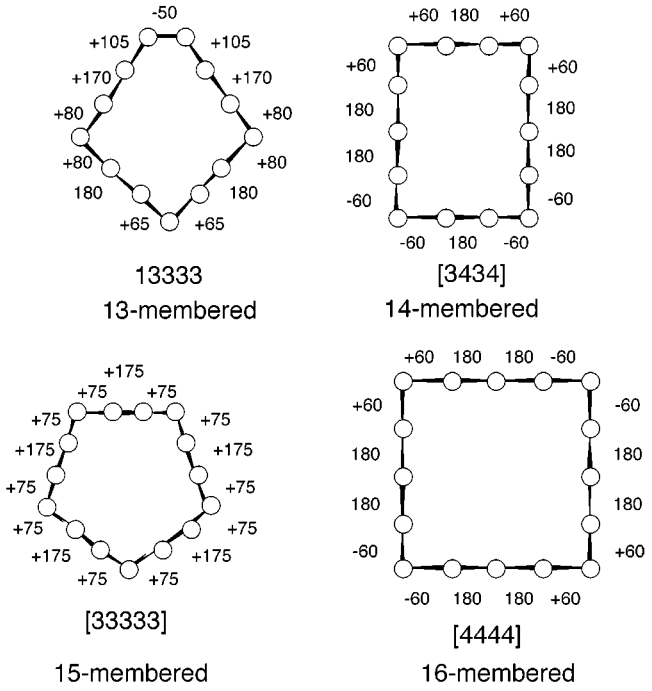

Figure 2. Calculated lowest energy conformations for cyclotridecane, cyclotetradecane, cyclopentadecane, and cyclohexadecane.[20,21] Numbers by bonds indicate the dihedral angle.

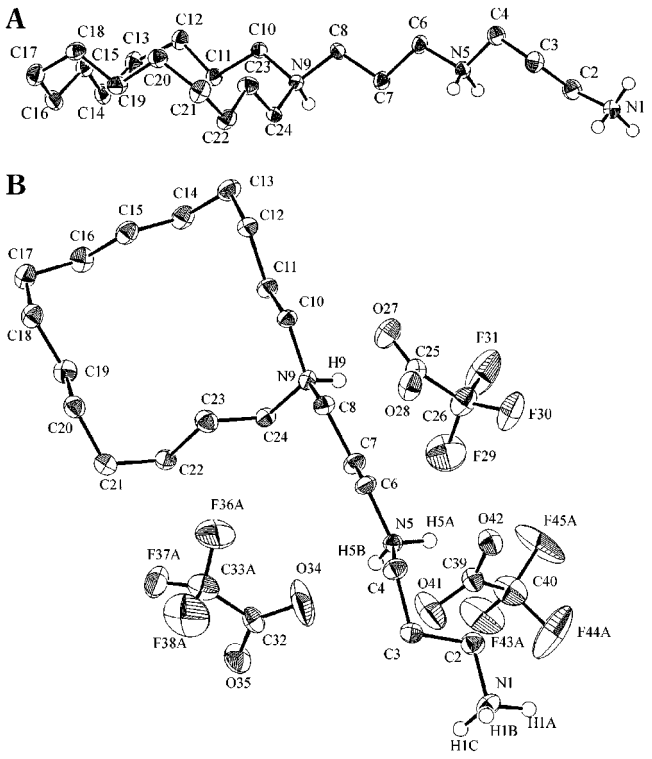

Figure 3. Computer-generated ORTEP drawings of the solid-state conformation of compound **20** as determined by single-crystal X-ray diffraction analysis. Panel **3A** is a side view. Panel **3B** is a top view.

lowest energy conformation for cyclohexadecane and the alkylated nitrogen atom occupies a corner position as in **47** and **48**. The spermidine-like side chain in **20** occupies a pseudoequatorial orientation with the N-9 to N-5 fragment extending one of the straight all anti sides of the macrocycle. As a result, the extended side chain and the macrocyclic amine form a very flat molecule in one of the dimensions as illustrated in the Figure 3A projection.

The striking agreement between the solid-state conformations of **47**, **48**, and **20** and the predicted lowest energy conformation based on Arnet's and Dale's calculations for the corresponding cycloalkanes suggested that a similar approach could be used to predict the lowest energy conformations of the motuporamine analogues having 14- and 15-membered saturated macrocyclic amines. Dale's analysis showed that for even-membered cycloalkanes the preferred conformations will be "quadrangular" diamond-lattice conformations, having four side units each consisting of straight all anti-chains joined together at right angles by a chain-bend element consisting of two gauche bonds of equal sign. If the ring is to remain even numbered, there are only four types of quadrangular conformations: all four sides contain an odd number of bonds, two adjacent or opposite sides contain an odd number of bonds and the others even, or all sides are even. For odd-membered rings it is impossible to have these four-sided structures. Instead, either three- or five-cornered conformations will be the best alternatives and give the least deformation at the corners. The three-sided type is called "triangular" and must have one or more concave sides. The five-sided conformations are called "quinquangular" and must have one or more concave sides. There are two types of triangular conformations: all three sides have an equal number of bonds or two sides are even and one is odd. There are four types of quinquangular conformations: all sides have an odd number of bonds, two adjacent or next-to-adjacent are even and the other three are odd, or one is odd and the other four are even.

Dale predicted that the lowest energy conformation for cyclotetradecane would be the [3434] conformation shown in Figure 2. This suggests that the lowest energy conformation of motuporamine B (**2**) would have the macrocyclic amine also in the [3434] conformation with the alkylated nitrogen at one of the four equivalent corners. The situation for dihydromotuporamine C (**13**) is somewhat more complex. Arnet has calculated that the lowest energy conformation for cyclopentadecane is the symmetrical [33333] conformer shown in Figure 2, but this conformation has a low entropy and, therefore, it is probably not favored at room temperature. Consequently, cyclopentadecane is predicted to exist as an interconverting mixture of the five low energy conformations [33333], [13443], [13434], [14334], and [13353] in solution at room temperature. A similar situation, where the alkylated nitrogen occupies corner positions in each conformer probably exists for dihydromotuporamine C (**13**). Indeed, since Dale and Arnet et al. predict that each of the cycloalkanes with ring sizes between 13- and 16-membered rings have a number of conformations that lie only 1−3 kcal/mol above the lowest energy conformation, it is most likely that all of the anti-invasive motuporamines **1**, **2**, **13**, **20**, and **21** exist as mixtures of interconverting conformations in solution at room temperature. This prediction would be consistent with the broad signals observed in the ^{1}H NMR spectra of all of these compounds.

Synthesis and Biological Activity of a Carbazole Analogue. Conformational analysis of the anti-invasive motuporamine **20** showed that the compound is almost planar in one dimension (Figure 2A) and predictions for

Chart 2. Structures of Motuporamine Analogs with Variations in the Side-Chain Fragment

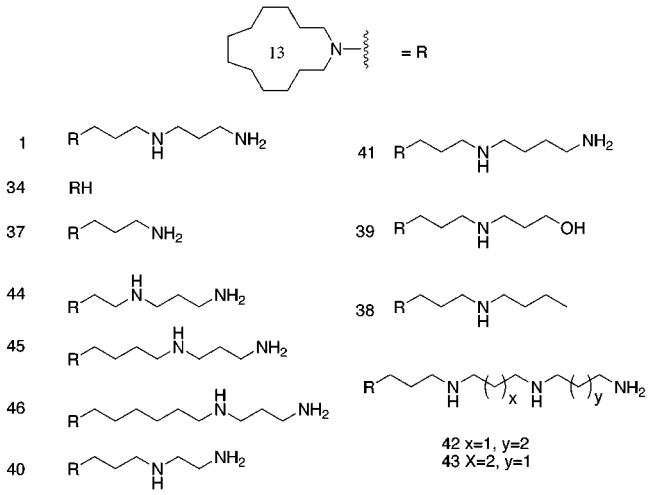

the conformations of the other active compounds suggest similar planar shapes. Figure 1A illustrates that in the series of motuporamines with saturated cyclic amine fragments there is no activity present in molecules with ring sizes of eleven atoms or smaller but that the naturally occurring 13-membered analogue motuporamine A (**1**) is active. Prompted by these two pieces of information about the motuporamine pharmacophore, we prepared the carbazole analogue **49**, which has a planar polycyclic aromatic amine fragment containing 12 carbons and one nitrogen like the macrocyclic amine fragment in motuporamine A (**1**). The analogue **49** was synthesized in a straightforward fashion according to the general pathway shown in Scheme 1A where carbazole was used in place of the saturated macrocylic amine component **I** and NaH was used as base to promote the Michael addition with methylacrylate. Compound **49** was more potent in the anti-invasion assay than was motuporamine A (**1**) and it was also more cytotoxic to MDA 231 cells than **1** (Figure 1A).

Discussion

Motuporamines A (**1**), B (**2**), and C (**3**) and G, H, and I (**15**) are a family of sponge alkaloids whose anti-invasive properties have been discovered by screening marine invertebrate extracts with a novel bioassay.[13] Further biological evaluation of motuporamine C (**3**), the most potent member of this natural product family in the anti-invasion assay, revealed that it was also active in a HUVEC in vitro sprouting assay and in a CAM in vivo assay for anti-angiogenic activity.[13] Motuporamine C (**3**) has been found to inhibit the motility of MDA-231 human breast cancer cells in vitro and it is believed that this is the basis of its anti-invasive and anti-angiogenic properties. The promising biological activities of the motuporamines combined with the relative simplicity and synthetic accessibility[15−17] of their structures makes them attractive candidates for preclincial evaluation as anti-angiogenic/anti-metastatic cancer drugs.

As a starting point in this process, the structural requirements for anti-invasion activity in the motuporamines have been explored by preparing a series of synthetic analogues and derivatives of the natural products (Charts 1 and 2). The solid bars in Figure 1A show the IC_{50} values for these compounds in the anti-invasion assay. Compounds **16**, **17**, **18**, **19**, **1**, **2**, **13**, **20**, and **21** form a series of motuporamines where the saturated cyclic amine fragment increases in size from 5 to 18 atoms. Figure 1A shows that motuporamines with cyclic amines having ring sizes of 11 atoms or less (**16**, **17**, **18**, and **19**) are all inactive in the assay, while motuporamines with ring sizes of 13 (**1**), 14 (**2**), 15 (**13**), 16 (**20**), and 18 (**21**) atoms are all active. Within the active group, the potency increases as the ring size increases from 13 to 15 atoms and then it decreases slightly as the ring size increases further to 16 and 18 atoms. The single methyl branches in the mixture of motuporamines G, H, and I (**15**) appears to increase the activity relative to the nonalkylated analogue motuporamine A (**1**). Comparison of the IC_{50}s for the pairs motuporamines B (**2**) and D (**4**), motuporamine C (**3**) and dihydromotuporamine C (**13**), and compounds **21** and **22** shows that the presence of a single *E* olefin in the macrocylic amine decreases the activity relative to the saturated analogue, with the effect being most dramatic in the smallest 14-membered ring. Similarly, the IC_{50}s for motuporamine E (**5**) and the analogue **23** suggest that the presence of a diene or a *Z* olefin in the macrocylic amine result in complete loss of activity.

Compounds **34** and **37**−**46** were prepared to explore the effect of changes in the spermidine-like side chain in motuporamine A (**1**). The data in Figure 1 shows that compounds having no side chain (**34**) or side chains containing only one amino functionality (**37**, **38**, and **39**) are all inactive. It was found that reducing the spacing between the macrocylic amine nitrogen and the first nitrogen in the tail to two methylenes (**44**) or increasing it to six methylenes (**46**) resulted in loss of activity, while a four methylene spacing (**45**) retained activity. Changing the spacing between the two distal nitrogens to either two (**40**) or four (**41**) methylenes gave active analogues as did extending the side chain to a triamine (**42**/**43**).

The series of acyclic compounds **26**, **27**, and **28** demonstrate that replacing the cyclic amine fragment of the active motuporamines with two alkyl chains of roughly comparable total carbon number results in active analogues. Most other variations in the macrocylic amine (i.e., **29**, **30**, **31** and **33**) led to inactive analogues. The one exception was the carbazole analogue **49**, which showed good activity.

One objective in the initial screen of crude extracts for anti-invasion activity was to remove cytotoxicity as a cause of invasion inhibition. Consequently, the assay was designed to eliminate any compounds that showed overt toxicity in the 2.5 h assay period. However, since the desired goal of anti-angiogenic and anti-metastatic therapies is to develop nontoxic drugs, the more stringent test of cytotoxicity after a 24h exposure to a particular compound has been applied to the active motuporamine analogues in order to evaluate their relative merits. All revealed some cytotoxicity after 24h but to different degrees. Figure 1 (lower panel) shows a plot of the ratios [IC_{50} for cytotoxicity versus MDA-231 cells/IC_{50} for inhibition of invasion by MDA-231 cells] for the compounds that showed anti-invasion activity at concentrations of <15 μM. The compounds with ratios of >1 have the desirable attribute of being more active in the anti-invasion assay than in the cytotoxicity assay. Only motuporamine B (**2**), motuporamine C (**3**), dihydromotuporamine C (**13**), the mixture of motuporamines G, H, I (**15**), and the carbazole analogue **49** have favorable

ratios of greater than 1, and among these dihydromotuporamine C (**13**) is both the most potent and has the most favorable ratio. The other active analogues, such as the acyclic compounds **26**, **27**, and **28**, all exhibit considerable cytotoxicity, making them of little interest as drug candidates. Figure 1 also shows the ratios [IC_{50} for cytotoxicity versus normal HUMEC breast cells/IC_{50} for inhibition of invasion by MDA-231 cells] for motuporamines A (**1**), B (**2**), and C (**3**) and dihydromotuporamine C (**13**), which illustrates that all of these compounds are less toxic to normal human breast cells than to the MDA-231 human breast cancer cells. In fact they showed no cytotoxicity to HUMEC cells at their IC_{50}s for anti-invasion activity. Dihydromotuporamine C (**13**) has the most favorable ratio for the anti-invasion activity HUMEC assay comparison, followed by motuporamine B (**2**), the motuporamine G, H, I mixture (**15**), and motuporamine A (**1**), again reflecting the optimization of properties as the cyclic amine ring size increases from 13 to 15 atoms.

The SAR data presented above show that the optimal structural requirements for maximum anti-invasion activity and minimum cytotoxicity in this family of alkaloids are a saturated monocyclic amine with ring sizes of 13, 14, or 15 atoms fused to a linear side chain containing two basic nitrogen atoms, where the spacing between each of the pairs of nitrogens is three methylene carbons. It is interesting to note that the natural motuporamines appear to have optimal structures for the desired combination of activities. Analysis of the conformations of motuporamines with 13-, 14-, 15-, and 16-membered macrocyclic amines suggests that the molecules exist as interconverting mixtures of quadrangular (even-numbered ring sizes) or quinquangular and triangular (odd-numbered ring sizes) conformers with the alkylated ring nitrogen atom occupying a pseudoequatorial corner position in each conformer resulting in an essentially flat molecule in one dimension. The carbazole analogue **49**, which was designed on the basis of the SAR and conformational features outlined above, showed good biological activity, indicating that other active analogues can be designed using this simple pharmacophore model. Preliminary testing of motuporamine C (**3**) against Lewis lung carcinoma in mice showed in vivo activity, which further highlights the anticancer potential of these interesting anti-invasive/anti-angiogenic alkaloids.[22]

Experimental Section

General Methods. ^{1}H chemical shifts are referenced to the residual MeOH-d_4 signal (δ 3.30 ppm) and ^{13}C chemical shifts are referenced to the MeOH-d_4 solvent peak (δ 49.5 ppm).

Isolation of the Natural Products. Specimens of *X. exigua* (Kirkpatrick)[1] were collected by hand using scuba at a depth of 15 m from vertical walls on the outer reef off Motupore Island, Papua New Guinea, in January 1995. A voucher sample has been deposited at the Zoological Museum of Amsterdam (ZMA POR 11521). Freshly collected sponge was frozen on site and transported to Vancouver over dry ice. A portion of the frozen sponge (86 g) was cut into small pieces and extracted repeatedly with MeOH (3 × 150 mL). The combined MeOH extracts were concentrated in vacuo and partitioned between EtOAc (3 × 70 mL) and H_2O (200 mL). The aqueous layer, which was active in the anti-invasion assay, was extracted with *n*-BuOH (3 × 70 mL) and the combined *n*-BuOH extracts were concentrated in vacuo to yield an anti-invasive brown oil (1.16 g). This oil was chromatographed repeatedly on Sephadex LH-20 with first MeOH (yielding 118.4 mg of active material) and then with 20:5:2 EtOAc/MeOH/H_2O as eluents to give a pale amorphous solid (55.6 mg) that stained red with ninhydrin and was active in the anti-invasion assay. The amorphous solid consisted of a mixture of a single class of alkaloids; the known motuporamines A−C (**1**−**3**), and the new motuporamines D (**4**), E (**5**), F (**6**), G (**15**), H (**15**), and I (**15**), plus additional uncharacterized analogues. Motuporamine C (**3**) was the major component (>90%).

It was possible to partially separate the motuporamine mixture at high dilution on HPLC (<0.3 mg per injection) using a semipreparative reversed-phase CSC−Inertsil 150A/ODS2, 5 μm 25 × 0.94 cm column, with 2% TFA in 3:2 MeOH/H_2O as eluent. This HPLC fractionation gave pure samples of motuporamines A (**1**), B (**2**), C (**3**), D (**4**), and E (**5**), a mixture of G, H, and I (**15**), and pure samples of monoacetylmotuporamine C (**7**) and monotrifluoroacetylmotuporamine C (**8**). Five additional motuporamines were collected, but in amounts insufficient for structure elucidation. Motuporamines G, H, and I (**15**) were obtained by first converting the mixture to the diacetamides by treatment with 1.5 mL of 3:1 pyridine/acetic anhydride with stirring at rt for 16 h. Evaporation of the reagents in vacuo gave a mixture of diacetylated products that were partially separated by semipreparative reversed-phase HPLC, using a CSC−Inertsil 150A/ODS2, 5 μm 25 × 0.94 cm column, with 0.39% TFA in 7:3 H_2O/MeCN as eluent. This HPLC fractionation gave a pure sample of diacetylmotuporamine G and a fraction containing a mixture of diacetylmotuporamines H and I. To obtain the natural products these two HPLC fractions were stirred at 98 °C for 16 h in 1N HCl. After which the samples were evaporated to dryness and further purified by semipreparative reversed-phase HPLC, using a CSC−Inertsil 150A/ODS2, 5 μm 25 × 0.94 cm column, with 2% TFA in 3:2 MeOH/H_2O as eluent to yield pure samples of motuporamine G (**15**), H (**15**) and I (**15**).

Except for motuporamine C (**3**), motuporamines A (**1**), B (**2**), D (**4**), E (**5**), **7**, **8**, G (**15**), H (**15**), and I (**15**) were isolated in submilligram quantities as the TFA salts. In a subsequent larger scale isolation the isolation procedure was improved by redissolving the active *n*-BuOH extract in H_2O and basifying with 5 N NaOH to pH >12 and then extracting with CH_2Cl_2. The active CH_2Cl_2 extract was then chromatographed as above. A total of 379.7 mg of motuporamines was isolated from 625 g of frozen sponge.

Motuporamine A (1): isolated as an oil; ^{1}H NMR, see Table 1; ^{13}C NMR, see Table 2; positive-ion HRFABMS [M + H]$^+$ *m/z* 298.3229 ($C_{18}H_{40}N_3$, calcd 298.3222).

Motuporamine B (2): isolated as an amorphous solid; ^{1}H NMR, see Table 1; ^{13}C NMR, see Table 2; positive-ion HRFABMS [M + H]$^+$ *m/z* 312.3387 ($C_{19}H_{42}N_3$, calcd 312.3379).

Motuporamine C (3): isolated as an amorphous solid; ^{1}H NMR, see Table 1; ^{13}C NMR, see Table 2; positive-ion HRFABMS [M + H]$^+$ *m/z* 324.3381 ($C_{20}H_{42}N_3$, calcd 324.3379).

Motuporamine D (4): isolated as an oil; ^{1}H NMR, see Table 1; ^{13}C NMR, see Table 2; positive-ion HRFABMS [M + H]$^+$ *m/z* 310.3212 ($C_{19}H_{40}N_3$, calcd 310.3222).

Motuporamine E (5): isolated as an oil; ^{1}H NMR, see Table 1; ^{13}C NMR, see Table 2; positive-ion HRFABMS [M + H]$^+$ *m/z* 322.3226 ($C_{20}H_{40}N_3$, calcd 310.3222).

Monoacetylmotuporamine C (7): isolated as an amorphous solid; ^{1}H NMR, see Table 1; ^{13}C NMR, see Table 2; positive-ion HRFABMS [M + H]$^+$ *m/z* 366.3484 ($C_{22}H_{44}N_3O$, calcd 366.3484).

Monotrifluoroacetylmotuporamine C (8): isolated as an amorphous solid; ^{1}H NMR, see Table 1; ^{13}C NMR, see Table 2; positive-ion HRFABMS [M + H]$^+$ *m/z* 420.3191 ($C_{22}H_{41}N_3OF_3$, calcd 420.3202).

Motuporamine G (15): isolated as an amorphous solid; ^{1}H NMR signals were very broad and the ^{13}C NMR was complex and had broad signals; ^{1}H NMR (400 MHz, MeOH-

(22) Roskelley, C.; Williams, D. E.; McHardy, L.; Andersen, R. J.; Roberge, M.; Troussard, A.; Leong, K.; Karsan, A.; Lee, T.; Minchinton, A.; Dedhar, S. *Proceedings of the 2001 AACR−NCI-EORTC International Conference, Published as a Supplement to Clinical Cancer Research*, **2001**, *7*(11), abstract #68.

d_4) δ 3.27 (m, 2H), 3.17 (m, 2H), 3.14 (m, 6H), 3.06 (t, J = 7.0 Hz, 2H), 2.18 (m, 2H), 2.09 (m, 2H), 1.77 (m, 4H), 1.66 (m, 1H), 1.58 (m, 1H), 1.53 (m, 1H), 1.40 (m, 11H), 1.28 (m, 1H), 0.97 (d, J = 6.2 Hz, 3H) ppm; positive-ion HRFABMS [M + H]$^+$ m/z 312.3387 ($C_{19}H_{42}N_3$, calcd 324.3379).

Motuporamine H (15): isolated as an amorphous solid; ^{1}H NMR signals were very broad and the ^{13}C NMR was complex and had broad signals; ^{1}H NMR (400 MHz, MeOH-d_4) δ 3.25 (m, 2H), 3.17 (m, 2H), 3.15 (m, 6H), 3.06 (t, J = 7.1 Hz, 2H), 2.18 (m, 2H), 2.09 (m, 2H), 1.77 (m, 4H), 1.54 (m, 4H), 1.41 (m, 9H), 1.20 (m, 2H), 0.91 (d, J = 6.3 Hz, 3H) ppm; positive-ion HRFABMS [M + H]$^+$ m/z 312.3387 ($C_{19}H_{42}N_3$, calcd 324.3379).

Motuporamine I (15): isolated as an amorphous solid; ^{1}H NMR signals were very broad and the ^{13}C NMR was complex and had broad signals; ^{1}H NMR (400 MHz, MeOH-d_4) δ 3.25 (m, 2H), 3.17 (m, 2H), 3.13 (m, 6H), 3.05 (t, J = 7.8 Hz, 2H), 2.17 (m, 2H), 2.09 (m, 2H), 1.78 (m, 4H), 1.54 (m, 2H), 1.40 (m, 9H), 1.27 (m, 2H), 1.16 (m, 2H), 0.92 (d, J = 6.5 Hz, 3H) ppm; positive-ion HRFABMS [M + H]$^+$ m/z 312.3382 ($C_{19}H_{42}N_3$, calcd 324.3379).

Acetylation of Motuporamine Mixture. The mixture of motuporamines (89.2 mg) was dissolved in 2 mL of 3:1 pyridine/acetic anhydride and stirred at rt for 16 h. Evaporation of the reagents in vacuo gave a mixture of diacetylated products that were partially separated by semipreparative reversed-phase HPLC, using a Whatman Magnum-9 Partisil 10 ODS-3 column, with 2:3 MeCN/(0.6% TFA/H_2O) as eluent. The previously described diacetylmotuporamines A (**10**) (eluting first) and C (**12**) (1.5 and 95.8 mg, respectively) were obtained as clear oils.[14] Three additional fractions were also obtained. The first of these, eluting after A (**10**), contained a mixture of diacetylmotuporamines D (**14**) and E. This fraction was further purified on reversed-phase HPLC, using a Whatman Magnum-9 Partisil 10 ODS-3 column, with 0.39% TFA in 35:65 MeCN/H_2O as eluent, to yield 1.2 mg of pure D (**14**) as a pale oil. The next eluting fraction, contained a mixture of diacetylmotuporamines B (**11**) and G, H and I, and was further fractionated on HPLC using the same conditions as for diacetylmotuporamine D (**14**) above. Pure diacetylmotuporamine B (**11**) (0.4 mg), pure diacetylated G (0.2 mg) and a fraction consisting of a mixture of diacetylated H and I (0.4 mg) were obtained. The slowest eluting fraction, eluting after diacetylmotuporamine C (**12**), was further purified using a Whatman Magnum-9 Partisil 10 ODS-3 column, with 0.39% TFA in 33:67 MeCN/H_2O as eluent, to yield 0.5 mg of diacetylmotuporamine F (**9**) as a clear oil. Additional diacetylmotuporamines were collected in each of the HPLC fractionations described but not enough material was obtained for complete characterization. Presumably all of the diacetylmotuporamines were isolated as the ammonium TFA salts.

Diacetylmotuporamine A (10) and C (12). Described previously.[14] The position of the $\Delta^{14,15}$ in **12** has subsequently been confirmed with the acquisition of well-resolved 2D-NMR data and has been unambiguously assigned through synthesis.[15−17]

Diacetylmotuporamine B (11). Previously described incorrectly while still a mixture with diacetylated motuporamines G, H, and I.[14] Identical to authentic synthetic diacetylmotuporamine B (**11**):[15] isolated as a pale clear oil; ^{1}H NMR, see Table 3 (Supporting Information); ^{13}C NMR, see Table 4 (see Supporting Information); positive-ion HRFABMS [M + H]$^+$ m/z 396.3580 ($C_{23}H_{46}N_3O_2$, calcd 396.3590).

Diacetylmotuporamine D (14): isolated as a clear oil; ^{1}H NMR, see Table 3 (Supporting Information); ^{13}C NMR, see Table 4 (Supporting Information); positive-ion HRFABMS [M + H]$^+$ m/z 394.3427 ($C_{23}H_{44}N_3O_2$, calcd 394.3434).

Diacetylmotuporamine F (9): isolated as a clear oil; ^{1}H NMR, see Table 1; ^{13}C NMR, see Table 2; positive-ion HRFABMS [M + H]$^+$ m/z 436.3538 ($C_{25}H_{46}N_3O_3$, calcd 436.3539).

Diacetylmotuporamine G: isolated as an oil; both the ^{1}H and ^{13}C NMR are very complex, this is attributed to a slow conformational equilibrium most likely involving the acetamide rotamers and ring dynamics; positive-ion HRFABMS [M + H]$^+$ m/z 396.3599 ($C_{23}H_{46}N_3O_2$, calcd 396.3590).

Diacetylmotuporamine H and I: isolated as an oil; positive-ion HRFABMS [M + H]$^+$ m/z 396.3582 ($C_{23}H_{46}N_3O_2$, calcd 396.3590).

Hydrogenation of Motuporamine C (3). A 6.4 mg (19.8 μmol) portion of motuporamine C (**3**) was dissolved in EtOH (1 mL) and reduced with H_2 gas on palladium/charcoal 10% catalyst with stirring overnight at rt. The reaction mixture was vacuum filtered through Celite and concentrated in vacuo. An HPLC pure sample of the pale amorphous TFA salt of **13** was prepared by semipreparative reversed-phase HPLC, using a CSC−Inertsil 150A/ODS2, 5 μm 25 × 0.94 cm column, with 2% TFA in 3:2 MeOH/H_2O as eluent (4.5 mg, 13.8 μmol, 70% yield).

Dihydromotuporamine C (13): isolated as an amorphous solid; ^{1}H NMR (400 MHz, MeOH-d_4) δ 3.24 (m, 2H), 3.10−3.21 (m, 8H), 3.05 (m, 2H), 2.17 (m, 2H), 2.08 (m, 2H), 1.72 (m, 4H), 1.46 (m, 8H), 1.36−1.42 (m, 12H) ppm; ^{13}C NMR (100 MHz, MeOH-d_4) δ 53.3, 52.9, 46.0, 46.0, 37.8, 27.7, 27.4, 27.4, 27.3, 25.5, 25.4, 22.9, 22.6 ppm; positive-ion HRFABMS [M + H]$^+$ m/z 326.3532 ($C_{20}H_{44}N_3$, calcd 326.3535).

Synthetic Analogues. General Procedures. Preparation of Macrocyclic Amines II from Lactams I (Scheme 1A). The 2-azacycloalkanones **I** (1.52 mmol) (2-azacyclotridecanone (**35**), 2-azacyclononanone, and 4-azatricyclo[4.3.1.1^{3,8}]-undecan-5-one) were reduced with LAH (1.3 mmol) in THF (7 mL) at 70 °C for 16 h. Excess LAH was quenched by slow dropwise addition of H_2O until a white precipitate formed. The resulting suspension was stirred for an additional 15 min and vacuum filtered through Celite, and the filtrate was acidified with 10% HCl to pH ∼2 and concentrated in vacuo. The resulting oil was partitioned between H_2O (15 mL, pH adjusted to >12 by addition of 1 N NaOH) and Et_2O (3 × 7 mL), the combined organic extracts were dried over $MgSO_4$ and filtered, and the Et_2O was removed by evaporation under a stream of N_2 to give macrocyclic amines **II** (e.g., **34**) (yield 98%).

Preparation of Motuporamines V and XI (e.g., 16, 17, 26, 27, 28, 29, 30, and 33, Schemes 1A and 3′b′). Secondary amines **II** (1.52 mmol) were reacted with methyl acrylate (1.6 mmol) in MeOH (10 mL) at rt for 16 h. After removal of the solvent and excess reagent in vacuo, the resulting β-amino ester **III** was reacted with a 10-fold excess of 1,3-diaminopropane or RNH_2 (ammonia (for compound **37**), ethylenediamine (for compound **40**), 3-aminopropanol (for compound **39**), 1,4-diaminobutane (for compound **41**), and spermidine (for compounds **42** and **43**)) in MeOH (10 mL) at rt for 4−5 d to give amides **IV**. Evaporation of the solvent and excess reagent in vacuo provided analytically pure amide. The amide was reduced with LAH (1.3 mmol) in THF (7 mL) at 70 °C for 16 h. The excess LAH was quenched by dropwise addition of H_2O until a white precipitate formed and the resulting suspension was stirred for 15 min. The slurry was vacuum filtered through Celite and the filtrate concentrated. Except in the case of compound **33**, the resulting oil was partitioned between H_2O (10 mL, pH kept at >12 by addition of 1N NaOH) and Et_2O (3 × 4 mL), the combined organic extracts were dried over $MgSO_4$ and filtered, and the solvent was removed in vacuo. In the case of compound **33,** the oil was instead acidified with 2 N HCl to pH 2, evaporated to dryness in vacuo and the resulting white solid suspended in MeOH and filtered. This filtrate was then subjected to HPLC purification as outlined below. The overall yield of the motuporamine analogues **V** and **XI** was 27−86%. An HPLC pure sample of the TFA salt of each analogue was obtained by semipreparative reversed-phase HPLC, using a Whatman Magnum-9 Partisil 10 ODS-3 column, with 2% TFA in 11:9−9:11 MeOH/H_2O as eluent.[23]

Conversion of Ketones VI to Lactams 1 (Scheme 1B). Hydroxylamine (0.68 g, 9.78 mmol) and sodium acetate (0.85 g, 10.36 mmol) were added to a solution of cyclodecanone (1.0 g, 6.48 mmol) or cyclopentadecanone (1.46 g, 6.48 mmol) in 50 mL of MeOH. The reaction mixtures were stirred for 1 h at rt. After removal of the MeOH under reduced pressure, the

(23) Goldring, W.; Hodder, A. S.; Weiler, L. *Tetrahedron Lett.* **1998**, *39*, 4955−4958.

remaining white powder was suspended in H_2O (75 mL) and extracted three times with Et_2O (30 mL). The combined organic extracts were dried over $MgSO_4$ and filtered, and the solvent was removed in vacuo to afford the oximes as white powders. The crude products were recrystallized from hexane to give the oximes as white needles in greater than 98% yield (HREIMS for cyclodecanone oxime $[M]^+ m/z$ 169.1471 ($C_{10}H_{19}NO$, calcd 169.1467) and for cyclopentadecanone oxime $[M]^+ m/z$ 239.2250 ($C_{15}H_{29}NO$, calcd 239.2249)).

To a solution of each of the oximes (6.37 mmol) in 50 mL of dry CH_2Cl_2 at 0 °C was added pyridine (1.03 mL, 12.74 mmol). Tosyl chloride was then added as a dry powder (1.58 g, 8.29 mmol) and the reaction was stirred overnight at rt. After removal of the solvent under reduced pressure the reaction products were dissolved in hexanes and loaded on a equilibrated 10 g silica sep pak. Flash chromatography using gradient elution from hexanes to 1:1 hexanes/EtOAc afforded a fraction from each reaction, eluting with 1:1 hexanes/EtOAc, that contained the lactams **I** as white needles in greater than 70% yield.

2-Azacycloundecanone: isolated as white needles; ^{1}H NMR (400 MHz, $CDCl_3$) δ 5.85 (bs, 1H), 3.28 (m, 2H), 2.17 (m, 2H), 1.70 (m, 2H), 1.56 (m, 2H), 1.45 (m, 4H), 1.32 (m, 4H), 1.28 (m, 2H) ppm; ^{13}C NMR (100 MHz, $CDCl_3$) δ 174.1, 39.6, 37.5, 26.8, 26.4, 26.4, 24.5, 23.7, 23.6, 23.2 ppm; HREIMS $[M]^+$ m/z 169.1468 ($C_{10}H_{19}NO$, calcd 169.1467).

2-Azacyclohexadecanone: isolated as white needles; ^{1}H NMR (400 MHz, $CDCl_3$) δ 6.09 (bs, 1H), 3.24 (m, 2H), 2.12 (t, J = 6.5 Hz, 2H), 1.57 (m, 2H), 1.41 (m, 2H), 1.22 (m, 20H) ppm; ^{13}C NMR (100 MHz, $CDCl_3$) δ 173.1, 38.8, 36.6, 29.2, 27.8, 27.6, 27.2, 27.1, 27.0, 26.3, 25.7, 25.7, 25.5, 25.4, 25.4 ppm; HREIMS $[M]^+$ m/z 239.2244 ($C_{15}H_{29}NO$, calcd 239.2249).

Preparation of Compound 21. Prior to HPLC purification, the mixture of compounds **22** and **23** (34.5 mg, 94.4 nmol) (obtained as described below) dissolved in EtOH (10 mL) was reduced with H_2 gas on palladium/charcoal 10% catalyst with stirring overnight at rt. The reaction mixture was vacuum filtered through Celite and concentrated in vacuo. An HPLC pure sample of the TFA/H_2O salt of **21** was prepared as described below.

Preparation of Compounds 22−25 (Scheme 2). DMF (120 μL, 1.54 mmol) and a 2.0 M solution of oxalyl chloride in CH_2Cl_2 (8.6 mL, 17.2 mmol) were sequentially added to a solution of undecylenic acid (2.86 g, 15.5 mmol) in CH_2Cl_2 (78.0 mL) at 0 °C, and the reaction was stirred for 1.5 h with slow warming to rt. The reaction was cooled to 0 °C, and NH_3 gas was bubbled into the solution with stirring for 20 min. The reaction was warmed to rt, diluted with EtOAc (70 mL), and sequentially washed with saturated $NaHCO_3$ solution, water, and brine (40 mL each). The combined aqueous layers were successively washed with EtOAc (3 × 40 mL). The combined organic layers were dried over $MgSO_4$, filtered, and concentrated in vacuo to afford undecyl-10-enamide (2.64 g, 93%) as a white solid (HREIMS $[M]^+$ m/z 183.1625 ($C_{11}H_{21}NO$, calcd 183.1623)).

8-Bromooctene (2.25 mL, 13.4 mmol) was added to a solution of undecyl-10-enamide (1.64 g, 9.0 mmol), crushed NaOH (1.26 g, 31.4 mmol), potassium carbonate (2.47 g, 17.9 mmol), and tetrabutylammonium hydrogen sulfate (0.30 g, 0.89 mmol) in toluene (15 mL), and the reaction was stirred for 1.5 h at 120 °C. The reaction was cooled to rt, diluted with CH_2Cl_2 (60 mL), and washed with H_2O (3 × 30 mL). The organic layer was dried over $MgSO_4$, filtered, and concentrated in vacuo. Purification of the residue by flash silica column chromatography using a step gradient of hexanes to 3:1 hexanes/EtOAc as eluent afforded *N*-(oct-7-enyl)-undecyl-10-enamide (1.60 g, 60%) as an amorphous white solid that was recrystallized from hexanes.

***N*-(Oct-7-enyl)undecyl-10-enamide:** isolated as white needles; ^{1}H NMR (400 MHz, $CDCl_3$) δ 6.23 (bs, 1H), 5.70 (m, 1H), 5.68 (m, 1H), 4.90 (d, J = 1.5 Hz, 1H), 4.86 (d, J = 1.5 Hz, 1H), 4.83 (s, 1H), 4.81 (s, 1H), 3.12 (m, 2H), 2.06 (t, J = 7.6 Hz, 2H), 1.93 (m, 4H), 1.52 (m, 2H), 1.40 (m, 2H), 1.26 (m, 4H), 1.22 (m, 4H), 1.19 (m, 8H) ppm; ^{13}C NMR (100 MHz, $CDCl_3$) δ 173.1, 138.8, 138.6, 114.1, 113.9, 39.2, 36.5, 33.6, 33.5, 29.4, 29.2, 29.2, 29.1, 28.9, 28.7, 28.6, 28.6, 26.6, 25.7 ppm; HREIMS $[M]^+ m/z$ 293.2719 ($C_{19}H_{35}NO$, calcd 293.2719).

A portion of the *N*-(oct-7-enyl)undecyl-10-enamide, obtained as white needles (220.9 mg, 0.75 mmol), was dissolved in sparged CH_2Cl_2 (50 mL) and along with a solution of Grubbs' benzylidene (31.3 mg, 37.9 μmole) in sparged CH_2Cl_2 (50 mL) it was added simultaneously to sparged CH_2Cl_2 (306 mL) over 3 h with stirring at 45 °C. After the addition, the reaction was stirred for an additional 3 h at 45 °C. The CH_2Cl_2 in the receiver flask was gently sparged with Ar gas during the addition and reaction. The reaction was cooled to rt, Et_3N (4 mL) was added, and the mixture was stirred for 15 min. The solution was concentrated in vacuo, and the resulting residue was purified by flash silica column chromatography using a step gradient of hexanes to EtOAc as eluent to give *E*/*Z*-2-azacyclooctadec-9-enone (166.5 mg, 83%, 2:1) as a white solid, and also a small quantity (12.5 mg, 23.5 μmol) of what was assumed to consist of a mixture of the four possible dimeric products of the ring-closing metathesis as a white solid.[15,23]

***E*/*Z*-2-Azacyclooctadec-9-enone:** isolated as white solid; ^{1}H NMR (400 MHz, $CDCl_3$) δ 6.12 (bs), 6.00 (bs), 5.17−5.37 (mregion), 3.14−3.23 (mregion), 2.10 (m), 1.91 (m), 1.56 (m), 1.41 (m), 1.20−1.26 (mregion) ppm; ^{13}C NMR (100 MHz, $CDCl_3$) δ 173.2, 173.0, 130.6, 130.5, 129.8, 129.7, 38.8, 38.6, 36.7, 36.5, 31.6, 31.4, 29.7, 29.5, 29.3, 29.1, 29.0, 28.9, 28.5, 28.4, 28.4, 28.2, 27.9, 27.5, 27.3, 27.1, 26.6, 26.2, 26.1, 26.0, 25.9, 25.7 ppm; HREIMS $[M]^+ m/z$ 265.2403 ($C_{17}H_{31}NO$, calcd 265.2406).

***E*/*Z*-2-Azacyclooctadec-9-enone dimer:** isolated as white solid; ^{1}H NMR (400 MHz, $CDCl_3$) δ 5.31 (m, 4H), 3.20 (m, 4H), 2.13 (m, 4H), 1.95 (m, 8H), 1.59 (m,4H), 1.46 (m, 4H), 1.26−1.34 (mregion, 28H) ppm; HREIMS $[M]^+$ m/z 530.4812 ($C_{34}H_{62}N_2O_2$, calcd 530.4811).

The *E*/*Z*-2-azacyclooctadec-9-enone and the mixture of dimeric products were reduced with LAH in THF (7 mL) as described above, and the resulting macrocyclic amines **IX** (Scheme 2) were converted to motuporamines using the chemistry outlined for the conversion of **III** to **V** in Scheme 1. A mixture of the *Z* and *E* analogues **22** and **23** (1:2) was first obtained by semipreparative reversed-phase HPLC, using a Whatman Magnum-9 Partisil 10 ODS-3 column, with 2% TFA in 7:3 MeOH/H_2O as eluent. An HPLC pure sample of the pale amorphous TFA/H_2O salt of the two analogues was then prepared by semipreparative reversed-phase HPLC, using a CSC−Inertsil 150A/ODS2, 5 μm 25 × 0.94 cm column, with 2% TFA in 7:3 MeOH/H_2O as eluent.

The mixture of dimeric products **24** and **25** were also obtained after the final LAH reduction of the resulting amides. No attempt was made to separate these by HPLC. Instead, these were isolated as the free base after the final ether extraction.

Preparation of Compound 38. To compound **37** (9.9 mg, 0.04 mmol) was added 1.5 mL of a 3:1 mixture of pyridine and butyric anhydride. The reaction was stirred overnight at rt. The solution was diluted with water (4 mL) and basified to pH 9 with 1 N NaOH and extracted with EtOEt (3 × 1.5 mL). The combined organic extracts were dried over $MgSO_4$ and filtered and the solvent removed in vacuo. The amide was reduced with LAH as described above.

Preparation of Compounds 44−46 (Scheme 3a). The macrocyclic amine **34** (1.52 mmol) was coupled with the methylhaloalkyl ester (1.57 mmol) (methylchloroacetate, methyl-4-iodobutyrate, and ethyl-6-bromohexanoate) in THF (12 mL) under reflux in the presence of Et_3N (4.56 mmol) for 3 h. After partition between H_2O (30 mL) and Et_2O (3 × 8 mL), the resulting ether-soluble α-, γ-, or ϵ-amino ester was reacted with a 10-fold excess of 1,3-diaminopropane and the resulting amide was reduced with LAH as described above to give the motuporamine analogues **XIII**.

Preparation of Compound 49. Carbazole (1.52 mmol) was dissolved in THF (10 mL) and NaH (1.56 mmol) added. The mixture was allowed to stir for 2 h at rt, and after the addition of methyl acrylate the reaction mixture was allowed to stir at rt for an additional 16 h. The excess NaH was quenched dropwise with H_2O and the reaction mixture extracted between

H_2O (22 mL) and Et_2O (3 × 7 mL). The resulting β-amino ester was then reacted with a 10-fold excess of 1,3-diaminopropane, and the resulting amide was reduced with LAH as described above to give the motuporamine analogue **49**.

Compound 16: isolated as an amorphous solid; ^{1}H NMR (400 MHz, MeOH-d_4) δ 3.67 (b, 2H), 3.30 (m, 2H), 3.07−3.17 (m, 6H), 3.05 (t, J = 7.6 Hz, 2H), 2.01−2.21 (m, 8H) ppm; ^{13}C NMR (100 MHz, MeOH-d_4) δ 55.3, 52.9, 45.9, 45.9, 37.8, 25.3, 24.0, 23.9 ppm; positive-ion HRFABMS [M + H]$^+$ m/z 186.1964 ($C_{10}H_{24}N_3$, calcd 186.1970).

Compound 17: isolated as an amorphous solid; ^{1}H NMR (400 MHz, MeOH-d_4) δ 3.53 (bd, J = 8.5 Hz, 2H), 3.11−3.21 (m, 6H), 3.05 (t, J = 6.1 Hz, 2H), 2.93 (bt, J = 9.2 Hz, 2H), 2.17 (m, 2H), 2.09 (m, 2H), 1.95 (m, 2H), 1.79 (m, 2H), 1.52 (m, 2H) ppm; ^{13}C NMR (100 MHz, MeOH-d_4) δ 54.8, 54.5, 46.0, 37.8, 25.4, 24.2, 24.2, 22.6, 22.1 ppm; positive-ion HRFABMS [M + H]$^+$ m/z 200.2128 ($C_{11}H_{26}N_3$, calcd 200.2127).

Compound 18: isolated as an amorphous solid; ^{1}H NMR (400 MHz, MeOH-d$_4$) δ 3.37 (m, 4H), 3.25 (m, 2H), 3.10−3.17 (m, 4H), 3.05 (bt, J = 7.8 Hz, 2H), 2.20 (m, 2H), 2.09 (m, 2H), 1.90 (m, 4H), 1.67 (m, 4H), 1.64 (m, 4H) ppm; ^{13}C NMR (100 MHz, MeOH-d_4) δ 54.3, 52.2, 46.0, 45.9, 37.8, 25.4, 25.1, 24.7, 22.8, 22.6 ppm; positive-ion HRFABMS [M + H]$^+$ m/z 242.2587 ($C_{14}H_{32}N_3$, calcd 242.2596).

Compound 19: isolated as an amorphous solid; ^{1}H NMR (400 MHz, MeOH-d_4) δ 3.29 (m, 4H), 3.25 (m, 2H), 3.13 (m, 4H), 3.06 (m, 2H), 2.18 (m, 2H), 2.09 (m, 2H), 1.87 (m, 4H), 1.53 (m, 6H), 1.50 (m, 6H) ppm; ^{13}C NMR (100 MHz, MeOH-d_4) δ 53.8, 53.6, 50.0, 45.9, 37.8, 25.9, 25.8, 25.3, 24.8, 23.0, 22.5 ppm; positive-ion HRFABMS [M + H]$^+$ m/z 270.2909 ($C_{16}H_{36}N_3$, calcd 270.2909).

Compound 20: isolated as cubic crystals; mp 168−171 °C; ^{1}H NMR (400 MHz, MeOH-d$_4$) δ 3.25 (m, 2H), 3.15 (m, 8H), 3.05 (t, J = 7.6 Hz, 2H), 2.18 (m, 2H), 2.09 (m, 2H), 1.69 (m, 4H), 1.45 (m, 10H), 1.37 (m, 12H) ppm; ^{13}C NMR (100 MHz, MeOH-d$_4$) δ 52.8, 52.7, 50.0, 45.9, 37.8, 27.7, 27.6, 27.6, 27.5, 27.1, 25.3, 25.2, 22.7, 22.5 ppm; positive-ion HRFABMS [M + H]$^+$ m/z 340.3684 ($C_{21}H_{46}N_3$, calcd 340.3692).

Compound 21: isolated as an amorphous solid; ^{1}H NMR (400 MHz, MeOH-d_4) δ 3.25 (bm, 2H), 3.17 (bm, 8H), 3.07 (bm, 2H), 2.17 (bm, 2H), 2.10 (bm, 2H), 1.71 (bm, 4H), 1.41 (bm, 10H), 1.34 (m, 16H) ppm; ^{13}C NMR (100 MHz, MeOH-d_4) δ 53.0, 52.5, 46.1, 46.0, 37.8, 28.8, 28.6, 28.5, 28.2, 28.1, 27.8, 26.4, 25.4, 23.5, 22.5 ppm; positive-ion HRFABMS [M + H]$^+$ m/z 368.3995 ($C_{23}H_{50}N_3$, calcd 368.4005).

Compound 22: isolated as an amorphous solid; ^{1}H NMR (400 MHz, MeOH-d_4) δ 5.36 (m, 2H), 3.25 (m, 2H), 3.14 (m, 8H), 3.05 (t, J = 7.6 Hz, 2H), 2.16 (m, 2H), 2.04−2.12 (m, 6H), 1.70 (m, 4H), 1.40 (m, 10H), 1.35 (m, 8H) ppm; ^{13}C NMR (100 MHz, MeOH-d_4) δ 131.3, 130.7, 53.3, 53.0, 52.7, 46.0, 45.9, 37.8, 30.2, 30.1, 29.2, 29.2, 29.1, 28.6, 28.2, 27.8, 27.8, 26.9, 25.9, 25.4, 24.3, 23.2, 22.4 ppm; positive-ion HRFABMS [M + H]$^+$ m/z 366.3844 ($C_{23}H_{48}N_3$, calcd 366.3848).

Compound 23: isolated as an amorphous solid; ^{1}H NMR (400 MHz, MeOH-d_4) δ 5.32 (m, 2H), 3.25 (m, 2H), 3.13 (m, 8H), 3.04 (t, J = 7.4 Hz, 2H), 2.16 (m, 2H), 2.08 (m, 2H), 2.00 (m, 4H), 1.67 (m, 4H), 1.31−1.43 (m, 18H) ppm; ^{13}C NMR (100 MHz, MeOH-d_4) δ 132.2, 131.9, 52.8, 52.4, 51.9, 46.0, 45.9, 37.8, 32.9, 32.9, 29.8, 29.7, 29.3, 29.0, 28.6, 28.4, 27.9, 26.6, 25.7, 25.3, 24.0, 22.6, 22.2 ppm; positive-ion HRFABMS [M + H]$^+$ m/z 366.3854 ($C_{23}H_{48}N_3$, calcd 366.3848).

Compounds 24 and 25: isolated as an amorphous solid; ^{1}H NMR (400 MHz, MeOH-d_4) δ 5.38 (m, 4H), 2.57 (m, 6H), 2.44 (m, 6H), 2.36 (m, 12H), 2.07−1.97 (m, 16H), 1.49 (m, 16H), 1.30 (m, 28H) ppm; ^{13}C NMR (100 MHz, MeOH-d_4) consisted of very broad and complex resonances with chemical shifts as expected; positive-ion HRFABMS [M + H]$^+$ m/z 730.7538 ($C_{46}H_{95}N_6$, calcd 730.7546).

Compound 26: isolated as an amorphous solid; ^{1}H NMR (400 MHz, MeOH-d_4) δ 3.23 (m, 2H), 3.13 (m, 6H), 3.05 (t, J = 7.8 Hz, 2H), 2.96 (tm, J = 7.8 Hz, 2H), 2.16 (m, 2H), 2.09 (m, 2H), 1.69 (m, 4H), 1.36 (m, 12H), 0.92 (t, J = 6.9 Hz, 6H) ppm; ^{13}C NMR (100 MHz, MeOH-d_4) δ 54.4, 50.8, 46.0, 45.9, 37.8, 32.4, 27.3, 25.4, 24.7, 23.5, 22.0, 14.2 ppm; positive-ion HRFABMS [M + H]$^+$ m/z 300.3378 ($C_{18}H_{42}N_3$, calcd 300.3379).

Compound 27: isolated as an amorphous solid; ^{1}H NMR (400 MHz, MeOH-d_4) δ 3.27 (m, 2H), 3.13 (m, 6H), 3.05 (t, J = 9.6 Hz, 2H), 2.96 (tm, J = 7.8 Hz, 2H), 2.15 (m, 2H), 2.09 (m, 2H), 1.68 (m, 4H), 1.36 (m, 4H), 1.30 (m, 16H) 0.89 (t, J = 6.5 Hz, 6H) ppm; ^{13}C NMR (100 MHz, MeOH-d_4) δ 54.4, 50.8, 46,0, 45.9, 37.8, 32.8, 30.2, 30.1, 27.6, 25.3, 24.7, 23.6, 22.0, 14.4 ppm; positive-ion HRFABMS [M + H]$^+$ m/z 356.3988 ($C_{22}H_{50}N_3$, calcd 356.4005).

Compound 28: isolated as an amorphous solid; ^{1}H NMR (400 MHz, MeOH-d_4) δ 3.25 (m, 2H), 3.13 (m, 6H), 3.05 (m, 2H), 2.96 (tm, J = 7.8 Hz, 2H), 2.14 (m, 2H), 2.11 (m, 2H), 1.68 (m, 4H), 1.36 (m, 4H), 1.29 (m, 24H) 0.89 (t, J = 6.7 Hz, 6H) ppm; ^{13}C NMR (100 MHz, MeOH-d_4) δ 54.3, 50.9, 46,0, 45.9, 37.8, 33.0, 30.6, 30.5, 30.4, 30.2, 27.6, 25.4, 24.7, 23.7, 22.0, 14.4 ppm; positive-ion HRFABMS [M + H]$^+$ m/z 412.4621 ($C_{26}H_{58}N_3$, calcd 412.4631).

Compound 29: isolated as an amorphous solid; ^{1}H NMR (400 MHz, MeOH-d_4) δ 7.28 (m, 3H), 7.20 (m, 1H), 4.49 (b, 2H), 3.62 (b, 2H), 3.41 (m, 2H), 3.15−3.24 (m, 6H), 3.06 (t, J = 7.6 Hz, 2H), 2.29 (m, 2H), 2.10 (m, 2H) ppm; ^{13}C NMR (100 MHz, MeOH-d_4) δ 132.0, 129.9, 129.6, 128.5, 128.4, 127.9, 54.3, 54.0, 51.4, 46.0, 45.9, 37.8, 26.2, 25.4, 22.4 ppm; positive-ion HRFABMS [M + H]$^+$ m/z 248.2131 ($C_{15}H_{26}N_3$, calcd 248.2127).

Compound 30: isolated as an amorphous solid; ^{1}H NMR (400 MHz, MeOH-d_4) δ 3.53 (bd, J = 11.8 Hz, 1H), 3.35 (2H), 3.08−3.21 (m, 5H), 3.05 (t, J = 7.6 Hz, 2H), 2.85 (tm, J = 11.0 Hz, 1H), 2.27 (m, 1H), 2.15 (m, 2H), 2.09 (m, 2H), 1.91 (m, 2H), 1.69−1.89 (m, 4H), 1.57 (m, 1H), 1.45 (m, 1H), 1.26−1.40 (m, 3H), 1.17 (m, 1H) ppm; ^{13}C NMR (100 MHz, MeOH-d_4) δ 68.7, 54.3, 50.2, 46.0, 46.0, 41.6, 37.8, 33.6, 30.7, 28.6, 26.1, 25.9, 25.3, 24.2, 21.2 ppm; positive-ion HRFABMS [M + H]$^+$ m/z 254.2585 ($C_{15}H_{32}N_3$, calcd 254.2596).

Compound 31: isolated as an amorphous solid; ^{1}H NMR (400 MHz, MeOH-d_4) δ 3.77 (m, 2H), 3.72 (m, 1H), 3.32 (m, 2H), 3.08−3.17 (m, 4H), 3.05 (bt, J = 7.6 Hz, 2H), 2.33 (m, 1H), 2.19 (m, 2H), 2.09 (m, 2H), 2.03 (m, 6H), 1.80 (m, 2H), 1.67 (m, 4H) ppm; ^{13}C NMR (100 MHz, MeOH-d_4) δ 62.2, 62.1, 55.9, 46.0, 46.0, 39.9, 37.8, 36.8, 35.2, 33.3, 31.7, 29.1, 27.0, 26.6, 25.3, 23.1 ppm; positive-ion HRFABMS [M + H]$^+$ m/z 266.2587 ($C_{16}H_{32}N_3$, calcd 266.2596).

Compound 33: isolated as an amorphous solid; ^{1}H NMR (400 MHz, MeOH-d_4) δ 3.81 (bs, 4H), 3.65 (bs, 12H), 3.47 (t, J = 4.8 Hz, 4H), 3.38 (m, 2H), 3.17 (t, J = 7.6 Hz, 2H), 3.15 (t, J = 7.6 Hz, 2H), 3.05 (t, J = 7.8 Hz, 2H), 2.21 (m, 2H), 2.10 (m, 2H) ppm; ^{13}C NMR (100 MHz, MeOH-d_4) δ 71.0, 70.5, 70.0, 55.5, 55.5, 52.8, 46.0, 45.9, 37.8, 25.4, 21.5 ppm; positive-ion HRFABMS [M + H]$^+$ m/z 334.2710 ($C_{16}H_{36}N_3O_4$, calcd 334.2706).

Compound 34: isolated as an oil; ^{1}H NMR (400 MHz, MeOH-d_4) δ 2.64 (t, J = 5.9 Hz, 4H), 1.55 (m, 4H), 1.39 (m, 16H) ppm; ^{13}C NMR (100 MHz, MeOH-d_4) δ 48.0, 28.1, 27.3, 27.0, 26.5, 25.4 ppm; positive-ion HRFABMS [M + H]$^+$ m/z 184.2069 ($C_{12}H_{26}N$, calcd 184.2065).

Compound 37: isolated as an amorphous solid; ^{1}H NMR (400 MHz, MeOH-d_4) δ 3.23 (m, 2H), 3.19 (m, 4H), 3.03 (t, J = 7.4 Hz, 2H), 2.11 (m, 2H), 1.77 (m, 4H), 1.49 (m, 4H), 1.41 (m, 12H) ppm; ^{13}C NMR (100 MHz, MeOH-d_4) δ 53.4, 53.2, 37.8, 26.7, 25.9, 25.6, 25.3, 23.7, 22.3 ppm; positive-ion HRFABMS [M + H]$^+$ m/z 241.2638 ($C_{15}H_{33}N_2$, calcd 241.2644).

Compound 38: isolated as an amorphous solid; ^{1}H NMR (400 MHz, MeOH-d_4) δ 3.23 (m, 4H), 3.16 (m, 2H), 3.09 (t, J = 6.4 Hz, 2H), 3.02 (t, J = 6.3 Hz, 2H), 2.13 (m, 2H), 1.77 (m, 4H), 1.67 (m, 2H), 1.42 (m, 18H), 0.99 (t, J = 7.4 Hz, 3H) ppm; ^{13}C NMR (100 MHz, MeOH-d_4) δ 53.4, 53.1, 48.9, 45.7, 29.3, 26.7, 25.9, 25.6, 25.3, 22.5, 22.4, 20.8, 13.9 ppm; positive-ion HRFABMS [M + H]$^+$ m/z 297.3277 ($C_{19}H_{41}N_2$, calcd 297.3270).

Compound 39. Partial conversion to the trifluoroacetate adduct occurred on concentration in vacuo after HPLC purification; hence, this compound was isolated as the free base since the final step, extraction and evaporation of the Et_2O, provided analytically pure product. isolated as an oil; ^{1}H NMR (400 MHz, MeOH-d_4) δ 3.61 (t, J = 6.3 Hz, 2H), 2.67 (t, J = 7.3 Hz, 2H), 2.62 (t, J = 7.4 Hz, 2H), 2.39 (m, 4H), 1.72 (quintet, J = 6.6 Hz, 2H), 1.66 (quintet, J = 7.1 Hz, 2H), 1.45 (m, 4H), 1.38 (m, 18H), ppm; ^{13}C NMR (100 MHz, MeOH-d_4)

δ 61.6, 55.0, 54.3, 49.4, 48.2, 33.1, 28.0, 27.2, 26.9, 26.8, 26.5, 26.5 ppm; positive-ion HRFABMS $[M + H]^+$ *m/z* 299.3058 ($C_{18}H_{39}N_2O$, calcd 299.3062).

Compound 40: isolated as an amorphous solid; ^{1}H NMR (400 MHz, MeOH-d_4) δ 3.37 (m, 4H), 3.27 (m, 2H), 3.19 (bt, J = 7.1 Hz, 6H), 2.21 (m, 2H), 1.78 (m, 4H), 1.50 (m, 4H), 1.41 (m, 12H) ppm; ^{13}C NMR (100 MHz, MeOH-d_4) δ 53.4, 53.1, 46.2, 46.0, 36.9, 26.7, 25.9, 25.6, 25.3, 22.6, 22.3 ppm; positive-ion HRFABMS $[M + H]^+$ *m/z* 284.3056 ($C_{17}H_{38}N_3$, calcd 284.3066).

Compound 41: isolated as an amorphous solid; ^{1}H NMR (400 MHz, MeOH-d_4) δ 3.25 (m, 4H), 3.05−3.13 (m, 6H), 2.96 (bt, J = 7.1 Hz, 2H), 2.17 (m, 2H), 1.76 (m, 8H), 1.38−1.54 (m, 16H) ppm; ^{13}C NMR (100 MHz, MeOH-d_4) δ 53.4, 53.1, 48.3, 45.8, 40.0, 26.7, 25.9, 25.6, 25.5, 25.3, 24.2, 22.5, 22.3 ppm; positive-ion HRFABMS $[M + H]^+$ *m/z* 312.3392 ($C_{19}H_{42}N_3$, calcd 312.3379).

Compound 42 and 43: isolated as an amorphous solid; ^{1}H NMR (400 MHz, MeOH-d_4) δ 3.25 (m, 4H), 3.11−3.18 (m, 6H), 3.06 (m, 4H), 2.96 (t, J = 7.1, 2H), 2.04−2.22 (m, 4H), 1.70−1.82 (m, 8H), 1.48 (m, 4H), 1.40 (m, 12H) ppm; ^{13}C NMR (100 MHz, MeOH-d_4) δ 53.4, 53.1, 48.2, 48.2, 45.9, 45.9, 45.8, 45.8, 45.7, 39.9, 37.8, 26.7, 25.9, 25.6, 25.5, 25.3, 25.3, 24.2, 24.2, 24.1, 22.5, 22.3 ppm; positive-ion HRFABMS $[M + H]^+$ *m/z* 369.3950 ($C_{22}H_{49}N_4$, calcd 369.3957).

Compound 44: isolated as an amorphous solid; ^{1}H NMR (400 MHz, MeOH-d_4) δ 3.56 (m, 4H), 3.19−3.27 (m, 6H), 3.06 (bt, J = 7.6 Hz, 2H), 2.11 (m, 2H), 1.79 (m, 4H), 1.49 (m, 4H), 1.40 (m, 12H) ppm; ^{13}C NMR (100 MHz, MeOH-d_4) δ 53.7, 51.5, 46.3, 43.3, 37.7, 26.8, 25.9, 25.6, 25.4, 25.2, 22.1 ppm; positive-ion HRFABMS $[M + H]^+$ *m/z* 284.3058 ($C_{17}H_{38}N_3$, calcd 284.3066).

Compound 45: isolated as an amorphous solid; ^{1}H NMR (400 MHz, MeOH-d_4) δ 3.22 (m, 2H), 3.16 (m, 2H), 3.03−3.14 (m, 8H), 2.08 (m, 2H), 1.82 (m, 2H) 1.79 (m, 6H), 1.47 (m, 4H), 1.40 (m, 12H) ppm; ^{13}C NMR (100 MHz, MeOH-d_4) δ 55.6, 53.2, 48.2, 45.8, 37.8, 26.7, 25.9, 25.6, 25.3, 25.3, 24.3, 22.5, 22.4 ppm; positive-ion HRFABMS $[M + H]^+$ *m/z* 312.3380 ($C_{19}H_{42}N_3$, calcd 312.3379).

Compound 46: isolated as an amorphous solid; ^{1}H NMR (400 MHz, MeOH-d_4) δ 3.22 (m, 2H), 3.11 (m, 6H), 3.04 (t, J = 7.7 Hz, 2H), 3.01 (t, J = 7.7 Hz, 2H), 2.07 (m, 2H), 1.75 (m, 8H) 1.42 (m, 20H) ppm; ^{13}C NMR (100 MHz, MeOH-d_4) δ 56.3, 53.2, 48.9, 45.8, 37.8, 27.0, 26.9, 26.9, 26.7, 25.9, 25.6, 25.3, 25.3, 25.1, 22.4 ppm; positive-ion HRFABMS $[M + H]^+$ *m/z* 340.3696 ($C_{21}H_{46}N_3$, calcd 340.3692).

Compound 49: isolated as an yellow amorphous solid; ^{1}H NMR (400 MHz, MeOH-d_4) δ 8.07 (d, J = 7.5 Hz, 2H), 7.52 (d, J = 7.9 Hz, 2H), 7.44 (t, J = 7.9 Hz, 2H), 7.20 (t, J = 7.5 Hz, 2H), 4.50 (t, J = 6.7 Hz, 2H), 2.94−3.04 (m, 6H), 2.27 (m, 2H), 1.97 (m, 2H) ppm; ^{13}C NMR (100 MHz, MeOH-d_4) δ 141.5, 127.0, 124.3, 121.3, 120.3, 109.7, 46.9, 45.8, 40.6, 37.7, 26.9, 25.3 ppm; positive-ion HRFABMS $[M + H]^+$ *m/z* 282.1972 ($C_{18}H_{24}N_3$, calcd 282.1970).

X-ray crystallographic analysis of (20): $C_{27}H_{48}N_3F_9O_6$, a = 9.440(2) Å, b = 12.658(1) Å, c = 15.612(2) Å, α = 75.437(7)°, β = 78.353(6)°, γ = 73.735(4)°, V = 1715.8(4) Å^3, space group P-1, Z = 2, ρ_{calc} = 1.32 g/cm^3, $R[I > 2\sigma(I)] = 0.059$, wR_2-[all data] = 0.150.

Data were collected on a Rigaku/ADSC CCD area detector with graphite-monochromated Mo Kα radiation, to a maximum 2θ value of 50.3° at −100 °C. Data were collected in 0.50° oscillations with 55 s exposures and were processed using the d*TREK program.[24] The structure was solved by direct methods,[25] and all non-hydrogen atoms were refined anisotropically. Two of the three TFA anions had disordered CF_3 groups which were modeled using restraints on all C−F bond lengths and F−C−F bond angles. All C−H hydrogens were included in calculated positions, while all N−H hydrogens were found in difference maps and refined isotropically. All calculations were performed using the teXsan[26] and SHELXL97.[27]

Acknowledgment. Financial support was provided by grants from the National Cancer Institute of Canada (R.J.A.), the Natural Sciences and Engineering Research Council of Canada (R.J.A.), and the Canadian Breast Cancer Research Institute (M.R.). Mike LeBlanc and the staff of the Motupore Island Research Station assisted in the collection of *X. exigua*. We thank Joanne Emerman (Anatomy Department, UBC) for the HUMEC cells and Hilary Anderson for critically reading the manuscript.

Supporting Information Available: Crystallographic information files for compound **20**. Tables of ^{1}H and ^{13}C NMR data for the diacetyl derivatives of the natural motuporamines. ^{1}H and ^{13}C NMR spectra for the natural products and the synthetic analogues. This material is available free of charge via the Internet at http://pubs.acs.org.

JO016101C

(24) *d*TREK*: Area Detector Software, Version 4.13, Molecular Structure Corp., 1996−1998.

(25) Altomare, A.; Burla, M. C.; Cammalli, G.; Cascarano, M.; Giacovazzo, C.; Guagliardi, A.; Moliterni, A. G. G.; Polidori, G.; Spagna, A. *J. Appl. Crystallogr.* **1999**, *32*, 115−119.

(26) Molecular Structure Corporation; Crystal Structure Analysis Package, 1985, 1992.

(27) SHELXL97: Sheldrick, G. M. University of Göttingen, Germany, 1997.